DEVELOPMENT OF A PLANAR EQUIANGULAR SPIRAL AMPLIFIER

J. L. Putz, et al

Varian Associates

Prepared for:

Army Electronics Command

September 1974

UNCLASSIFIED

SECURITY CLASSIFICATION OF THIS PAGE *(When Data Entered)*

REPORT DOCUMENTATION PAGE		READ INSTRUCTIONS BEFORE COMPLETING FORM
1. REPORT NUMBER ECOM-73-0148-F	2. GOVT ACCESSION NO.	3. RECIPIENT'S CATALOG NUMBER AD-787339
4. TITLE *(and Subtitle)* DEVELOPMENT OF A PLANAR EQUIANGULAR SPIRAL AMPLIFIER		5. TYPE OF REPORT & PERIOD COVERED Final Report 1 April 1973 to 31 May 1974
		6. PERFORMING ORG. REPORT NUMBER
7. AUTHOR(s) J. L. Putz and A. W. Scott		8. CONTRACT OR GRANT NUMBER(s) DAAB07-73-C-0148
9. PERFORMING ORGANIZATION NAME AND ADDRESS Varian Associates 611 Hansen Way Palo Alto, California 94303		10. PROGRAM ELEMENT, PROJECT, TASK AREA & WORK UNIT NUMBERS
11. CONTROLLING OFFICE NAME AND ADDRESS U.S. Army Electronics Command AMSEL-TL-BM Fort Monmouth, New Jersey 07703		12. REPORT DATE September 1974 13. NUMBER OF PAGES 57
14. MONITORING AGENCY NAME & ADDRESS *(if different from Controlling Office)* Same		15. SECURITY CLASS. *(of this report)* UNCLASSIFIED 15a. DECLASSIFICATION/DOWNGRADING SCHEDULE N/A

16. DISTRIBUTION STATEMENT *(of this Report)*

Approved for public release; distribution unlimited.

17. DISTRIBUTION STATEMENT *(of the abstract entered in Block 20, if different from Report)*

18. SUPPLEMENTARY NOTES

19. KEY WORDS *(Continue on reverse side if necessary and identify by block number)*

radial-beam traveling wave tube; planar equiangular spiral amplifier

20. ABSTRACT *(Continue on reverse side if necessary and identify by block number)*

Work accomplished on the development of a radial-beam traveling wave tube is described. This report covers the period from 1 April 1973 to 31 May 1974. The tube is being developed to meet the requirements of U.S. Army Electronics Command Technical Guideline MW-89B under Contract DAAB07-73-C-0148.

The rf circuit used consists of a pair of planar equiangular (logarithmic) bifilar spirals deposited on ceramic substrates and placed on either side of a thin flat electron beam which expands radially from

DD FORM 1 JAN 73 1473

UNCLASSIFIED

SECURITY CLASSIFICATION OF THIS PAGE *(When Data Entered)*

20. ABSTRACT *(Continued)*

a ring-shaped cathode. A detailed analysis of the circuit properties and the wave-beam interaction is presented. A rough design procedure is also given based on certain reasonable assumptions. A computer program has been developed to aid in optimizing designs.

Experimental data from three tubes are presented, in the frequency range 0.5 to 1.0 GHz. Practical problems prevented operation of these tubes at the design beam current, but the results obtained indicated that the originally estimated impedance of the spiral circuits was too high by a considerable factor. When corrected for impedance, the theoretical gain predictions agreed fairly well with measured values at the low end of the frequency range, but were optimistic at the high end.

TABLE OF CONTENTS

1.0 INTRODUCTION

The purpose of this program was to demonstrate the feasibility of a new form of traveling wave interaction, using radially-directed waves and beams. A tube constructed on such principles shows considerable promise for wideband, medium-power, low-voltage applications.

The particular tube used in this investigation uses as the slow-wave circuit a pair of planar two-arm equiangular (logarithmic) spirals deposited on BeO ceramic substrates. A thin "sheet" electron beam from a cylindrical cathode is focused between the spiral circuits by means of a radial magnetic field. The electrons and rf signals travel outward together, and amplification of the signals takes place in essentially the same manner as in linear-beam TWTs. Ideally, the ceramic substrates can serve as part of the vacuum envelope, but in the present program, an external metal envelope was provided. A cross-sectional drawing of a typical tube is shown in Figure 1. Photographs of the tube and focusing structure are shown in Figures 2 to 4.

Objective specifications for the final phase of the program were as follows:

Rf power output	500 W cw minimum
Small-signal gain	20 dB
Efficiency	30%
Frequency range	0.5 to 1.0 GHz
Beam voltage	300 V maximum
Insertion loss	3 dB maximum
VSWR (cold)	1.5:1 maximum
Beam transmission	90% minimum
Modulating electrode	nonintercepting type

This report presents experimental results from three tubes, and a comprehensive theoretical analysis of radial wave-beam interaction, together with design procedures.

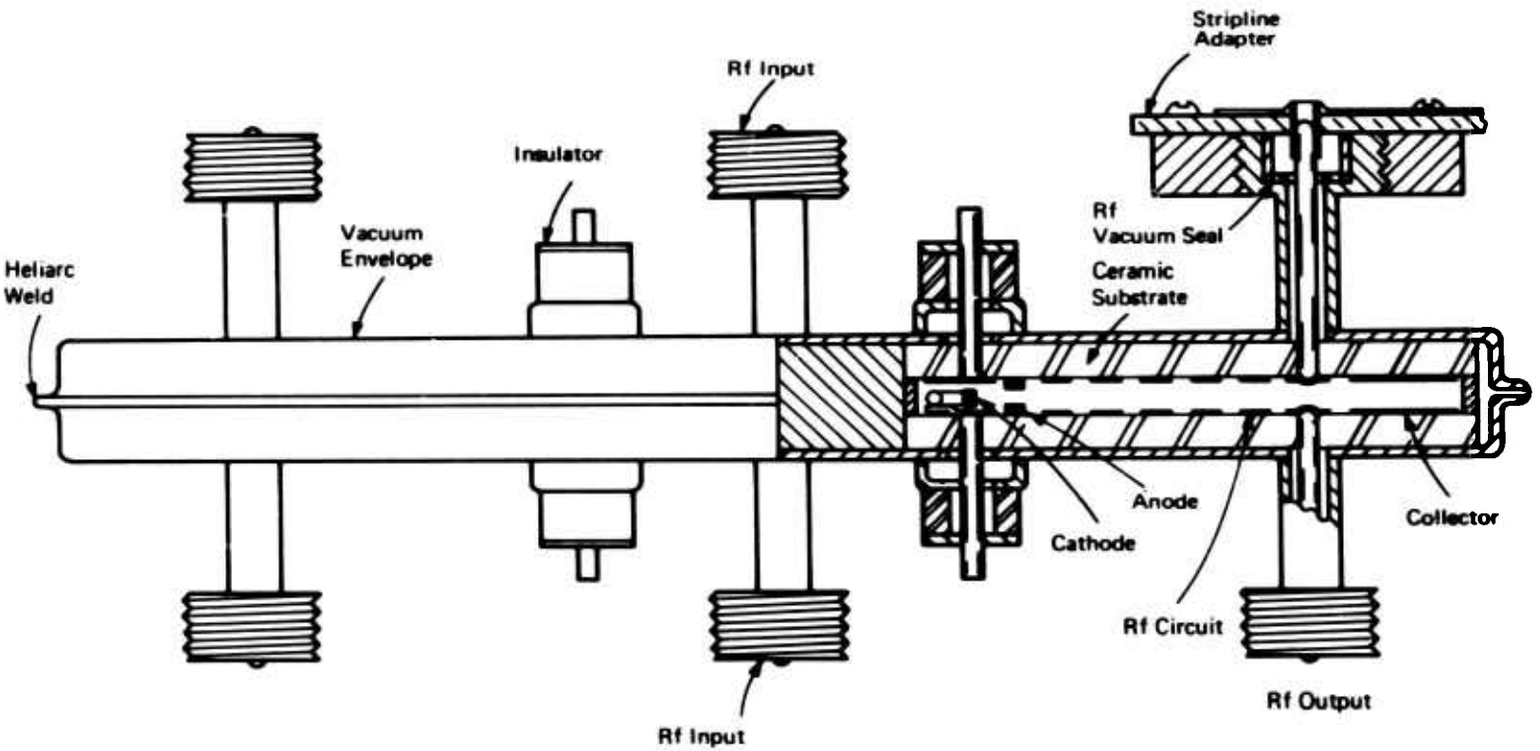

TP A-9308

A-9308

Figure 1. Cross Section of Radial Beam TWTs Serial No. 2 and 3

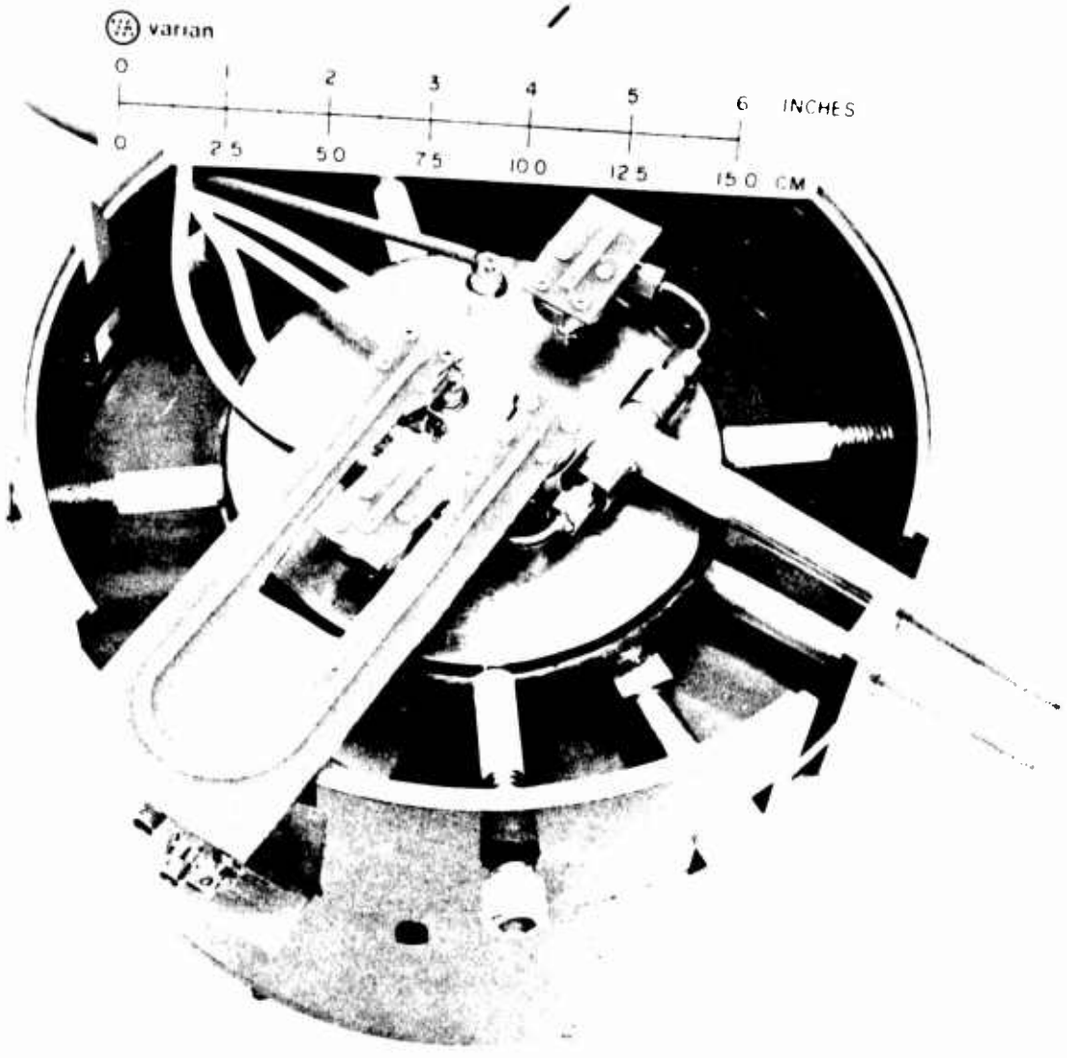

Neg. No. 36662-5

Figure 2. Radial Beam TWT No. 2 in Focusing Magnet

Neg. No. 36662-7

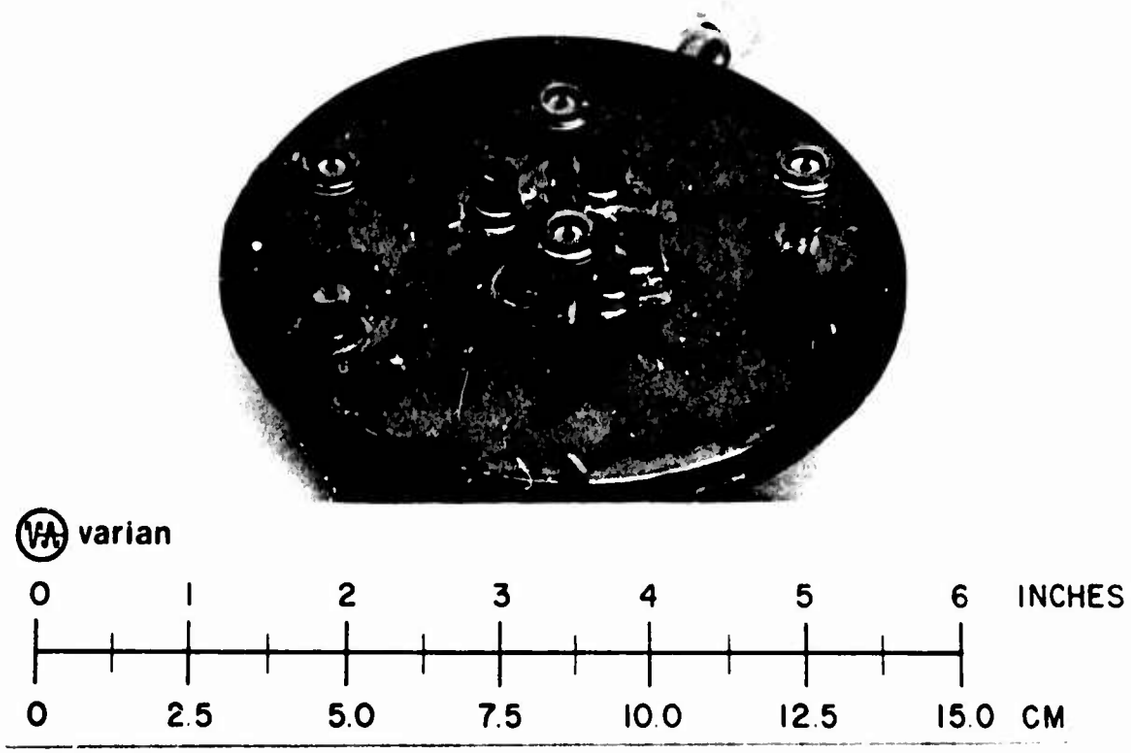

Figure 3. Radial-Beam TWT No. 2

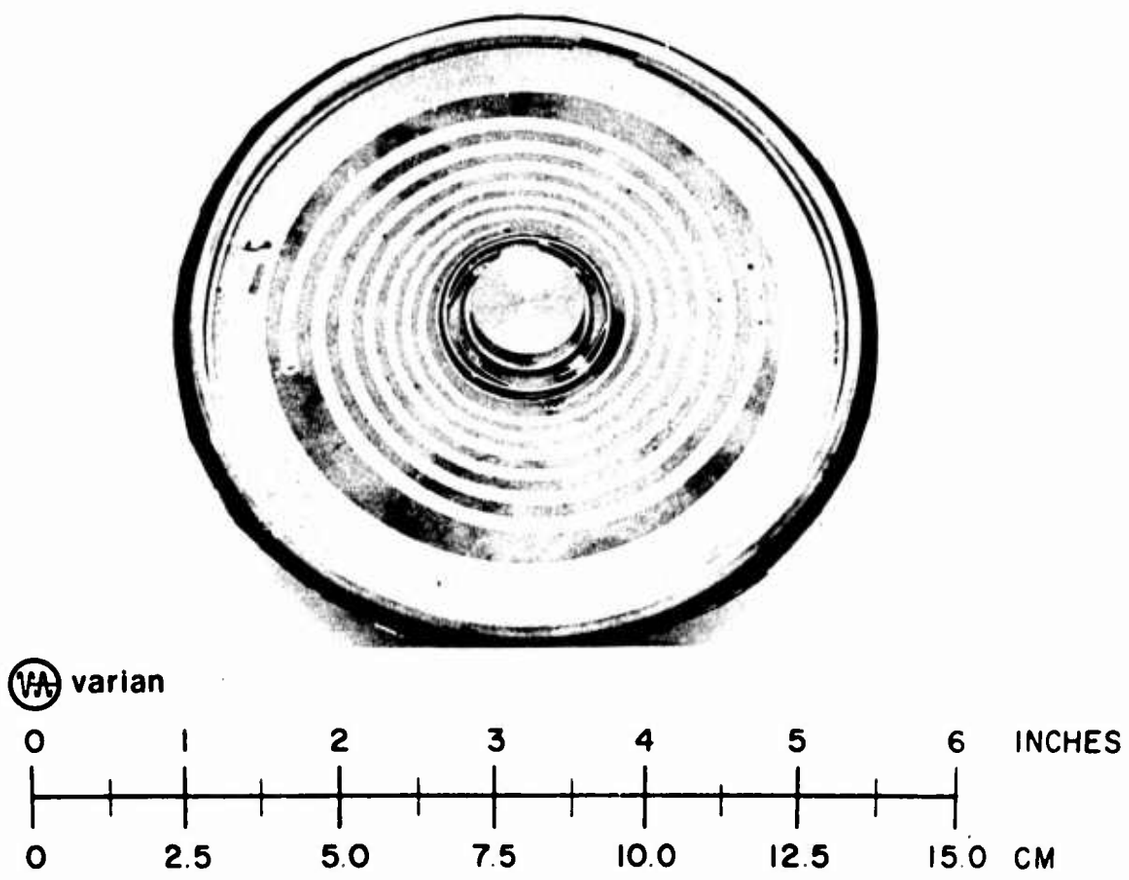

Figure 4. Slow-Wave Spiral Circuit and Electron Gun of Radial-Beam TWT No. 2

2.0 THEORY OF OPERATION

The performance of a radial-beam TWT (RBTWT) can be analyzed in two steps, in a manner similar to that used for a "developed" helix and sheet beam.[1] First, the characteristics of the rf circuit are found, and then the interaction of the beam and circuit are determined. Expressions for gain can then be written, and power output estimated. By combining these expressions with others arising from practical focusing considerations, a design procedure can be arrived at.

2.1 GAIN

The principal slow-wave characteristics of the logarithmic spiral can be obtained by analyzing the properties of a "spiral sheet," analogous to the way that the characteristics of a wire helix are obtained from a "sheath helix" model. The analysis has been carried out for the general configuration of Figure 5, which shows the arrangement of the circuits, support dielectrics, shields, and the electron beam. Details of the analysis are given in Appendix A. The normalized calculated phase velocity and impedance are shown in Figures 6 and 7 for BeO substrates of various thicknesses. The abscissa in Figure 6 is proportional to frequency.

The impedance K is the usual Pierce impedance parameter:

$$K = \frac{E_c^2}{2\gamma^2 P} \tag{2-1}$$

where:

E_c = value of the radial electric field at the circuit ($z = \ell$)
γ = radial propagation constant = $2\pi f/v_p$
P = power flowing radially along the circuits

For an electron beam of finite thickness, the effective impedance is smaller than the above value by a factor of:

$$\frac{K_{av}}{K_{ckt}} = \frac{1}{2\cosh^2(\beta\ell)}\left[\frac{\sinh(\beta t)}{\beta t} + 1\right] \tag{2-2}$$

where:

$\beta = \sqrt{\gamma^2 - k^2}$
$k^2 = \omega^2 \mu \epsilon_o$

For slow waves, $\beta \simeq \gamma$. Values from Eq. (2-2) are shown in Figure 8.

Figures 6 and 7 show that although the phase velocity is independent of radius, the impedance is inversely proportional to radius. Thus, there is no fixed rate of gain as in a linear-beam TWT. The total gain is best expressed in integral form as follows:

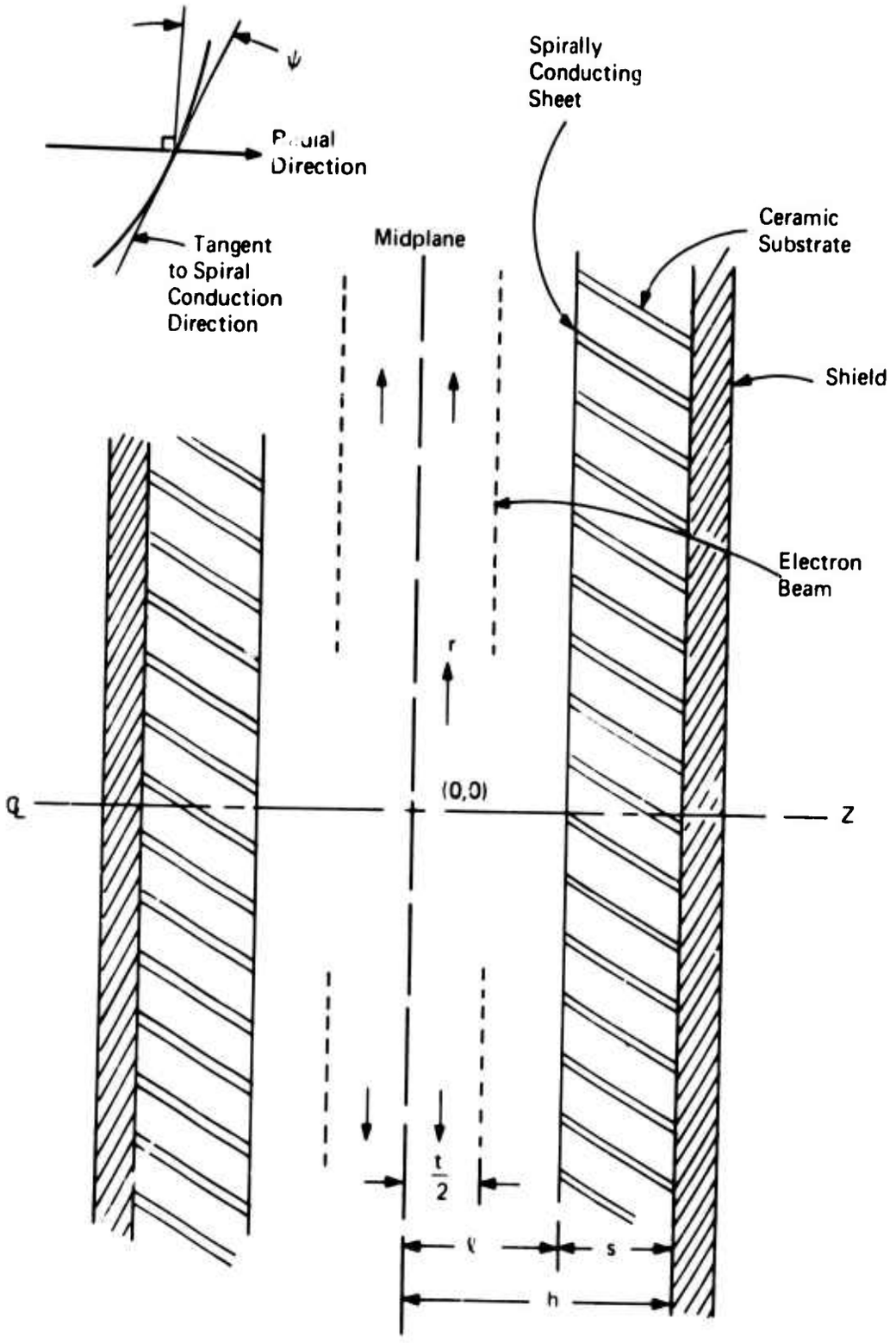

Figure 5. Analytical Model for a RBTWT

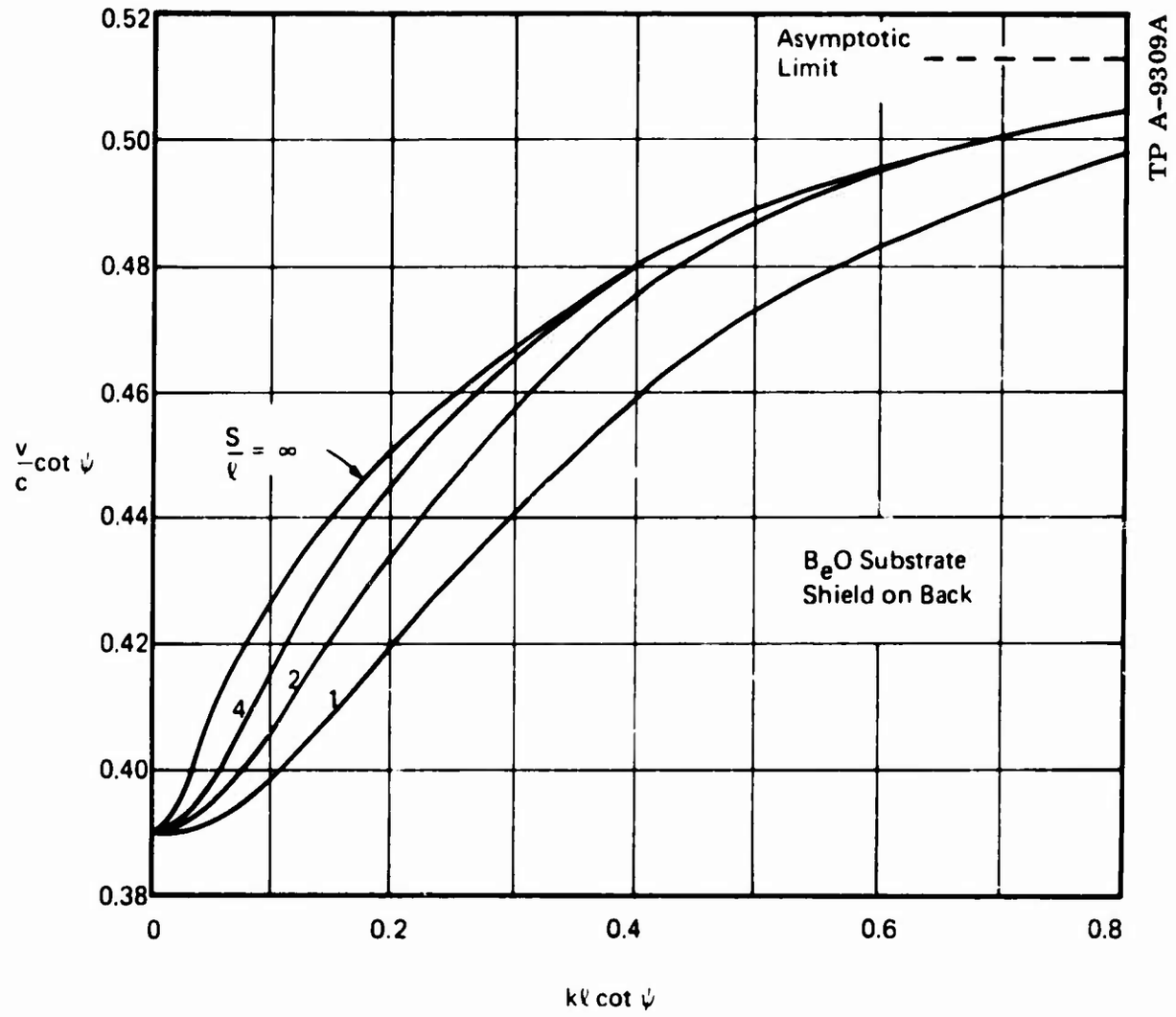

Figure 6. Phase Velocity of a Pair of Flat Spiral Circuits

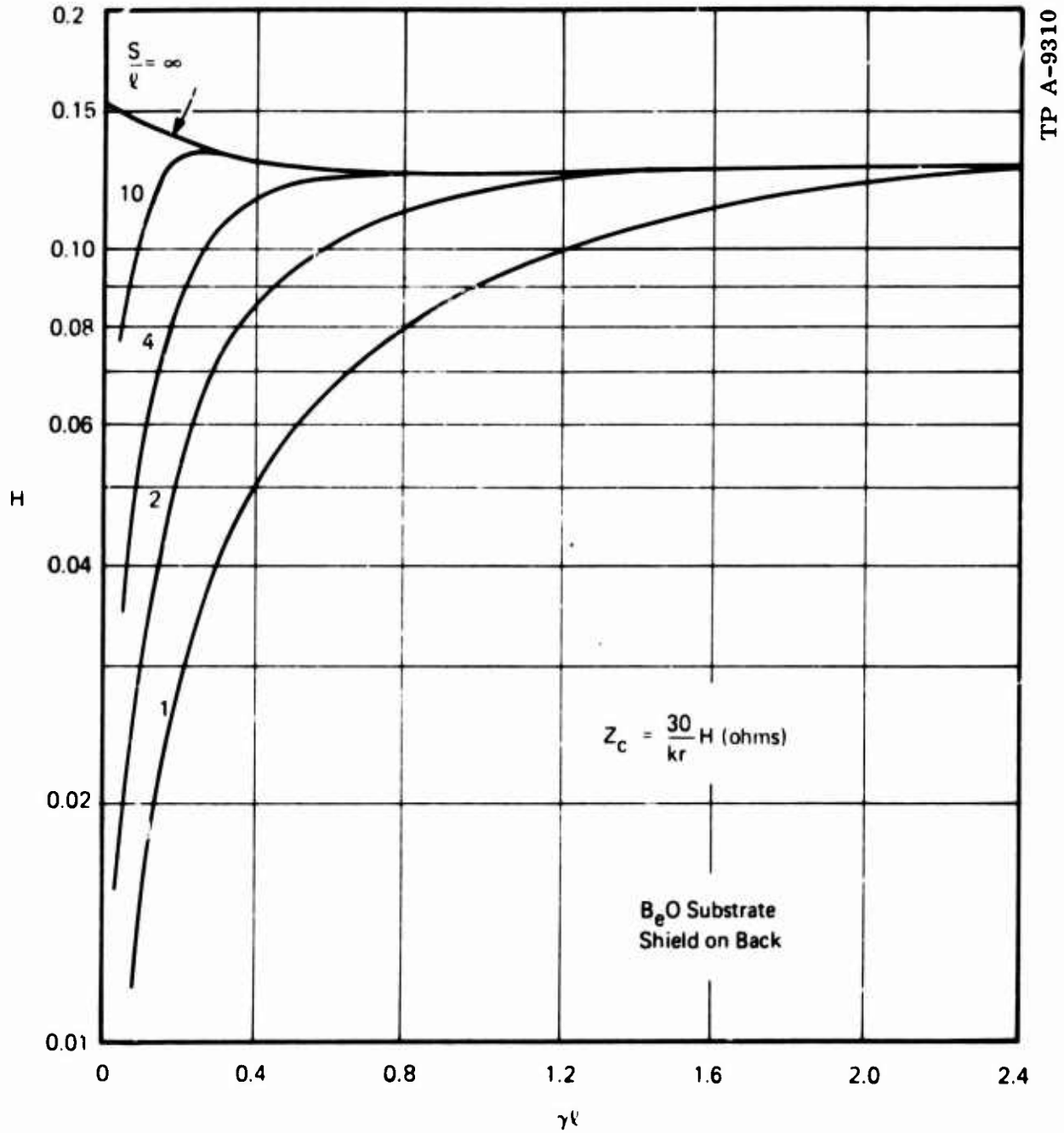

Figure 7. Impedance of a Pair of Flat Spiral Circuits

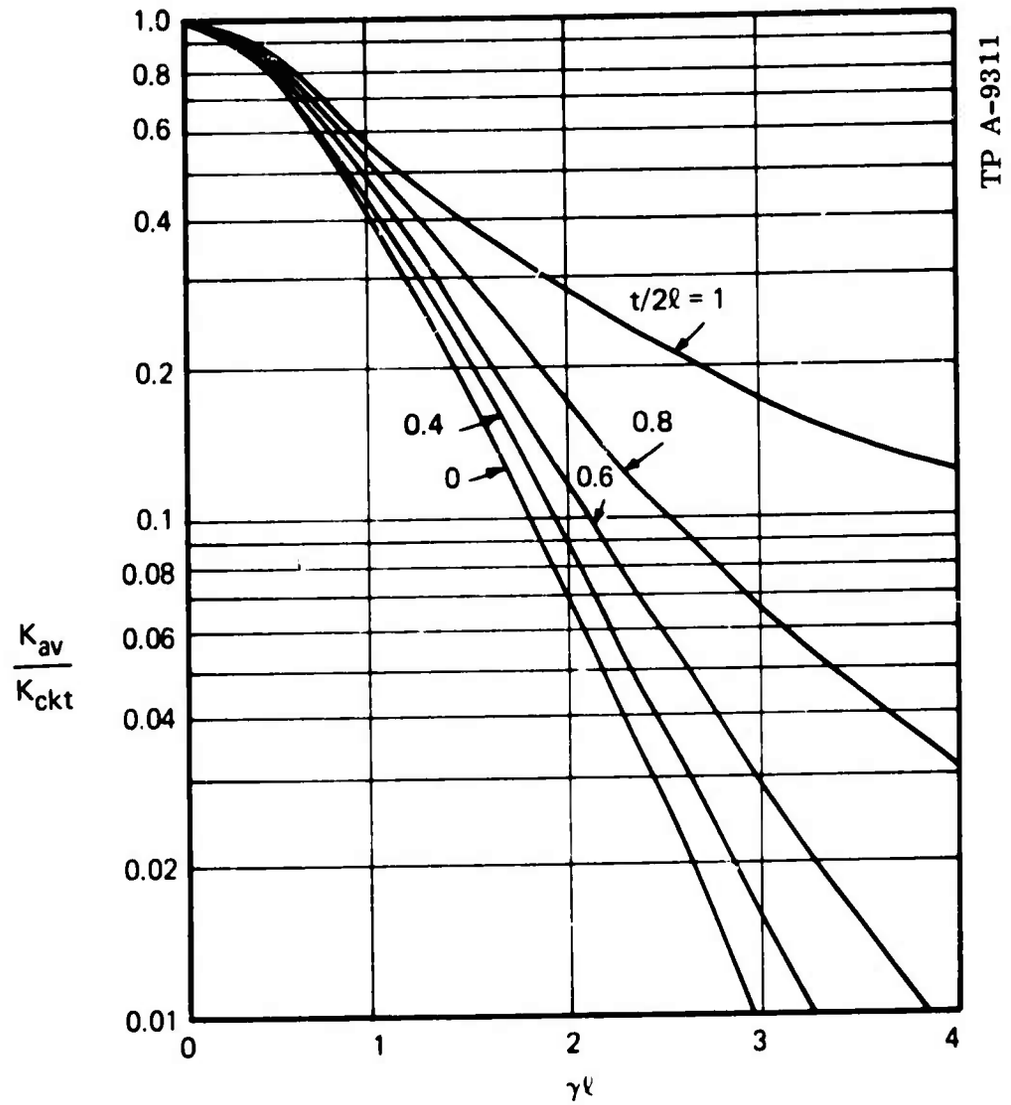

Figure 8. Impedance Reduction Factor for a Sheet Beam

$$E_{out} = E_{in} \exp\left(-\int_{r_1}^{r_2} \Gamma(r)\, dr\right) \tag{2-3}$$

where Γ is the complex propagation constant in the presence of the beam. As in the linear-beam TWT, there are three values of Γ, corresponding roughly to the circuit wave and the two space-charge waves in the beam. (In the RBTWT, the space-charge wavelength varies with radius.) The function $\Gamma(r)$ can be expressed in terms of an incremental propagation constant $\delta(r)$ as follows:

$$\Gamma(r) = j\beta_e\,[1 + jC\delta(r)] \tag{2-4}$$

where:

β_e = $2\pi f$/(dc beam velocity)

C = Pierce gain parameter

$$= \left[\frac{KI_o}{4V_o}\right]^{1/3} \tag{2-5}$$

I_o and V_o are the dc beam current and effective voltage, respectively. A detailed derivation of the relationship of $\delta(r)$ to the beam and circuit parameters is given in Appendix B.

In terms of the three incremental propagation constants, the power gain can be expressed as:

$$\text{Power gain} = \left|\frac{E_{out}}{E_{in}}\right|^2 \cdot \frac{r_2}{r_1} = \left|\frac{\sum_{n=1}^{3} E_n \exp\left(\int_{r_1}^{r_2} \beta_e C\delta_n(r)\, dr\right)}{E_T}\right|^2 \frac{r_2}{r_1} \tag{2-6}$$

where:

E_n = initial value of each of the three waves in turn

E_T = their sum

Expressions for E_n in terms of the δ's and the circuit and beam parameters are given in Appendix B.

Since one of the δ's (e.g., δ_1) usually has a larger real part than the others, the field component associated with this value of δ will eventually predominate if the circuit is long enough in the radial direction. In this case, the "one-wave" gain is given by:

$$\text{Gain (dB)} = A + 8.68 \int_{r_1}^{r_2} \beta_e C \quad Re\ \delta_1(r)\, dr + 10 \log\left(\frac{r_2}{r_1}\right) \tag{2-7}$$

where A is the "launching loss":

$$A = 20 \log \left| \frac{E_1}{E_T} \right| \tag{2-8}$$

A discussion of the value of A for various conditions is given in Appendix B. It may vary from as little as −3 dB to greater than −25 dB. An average value for normal operation is about −10 dB.

2.2 POWER

To estimate the power output of a spiral TWT, some assumption must be made as to efficiency. Since the wave-beam interaction mechanism is essentially the same as that in a linear-beam TWT, it seems reasonable to assume that the efficiency will be of order $2C_2$, where C_2 is evaluated using the interaction impedance at the output end of the circuit. Thus, the estimated power output is:

$$P_{out} = 2I_o V_o C_2 \tag{2-9}$$

2.3 VELOCITY SPREAD

In any small radial distance, the electron beam can be treated as a section of a strip beam. The velocity spread in a strip beam depends on the perveance "per square" (i.e., the perveance based on the current in a beamwidth equal to its thickness).[2]

In terms of the current density from a cylindrical cathode, the perveance per square at the input to the circuit is given by

$$S = 6.45 \frac{J_o t^2}{V_e^{3/2}} \cdot \frac{r_c}{r_1} \tag{2-10}$$

where:

J_o = cathode current density, in A/cm^2
t = beam thickness, in inches
r_c = cathode radius
V_e = voltage at the beam edge

For velocity spreads less than 20%, an approximate relationship between velocity spread and perveance per square is given by:

$$m \simeq 1 - \left(\frac{S}{70}\right) \times 10^6 \tag{2-11}$$

where m is the ratio of the lowest to the highest electron velocity in the beam. Equation (2-11) shows that if the velocity spread is to be less than 10%, S must be less than 7×10^{-6}.

In a dense strip beam, a voltage difference also exists between the beam edge and the surrounding circuit due to space-charge effects. This voltage depression can be expressed in terms of the velocity spread as follows:

$$\Delta V \simeq 2V_e(1-m^2)(2\ell/t-1) \tag{2-12}$$

Assuming that the effective beam voltage is the average of the voltages at the beam edge and at the midplane, the ratio of the effective beam voltage to the circuit voltage can be written as:

$$\frac{\bar{V}}{V_{ckt}} \simeq \frac{1+m^2}{2+4(1-m^2)(2\ell/t-1)} \tag{2-13}$$

For a maximum velocity spread of 10%, Eq. (13) reduces to:

$$\frac{\bar{V}}{V_{ckt}} = \frac{0.905}{1+0.38(2\ell/t-1)} \tag{2-14}$$

The above analysis indicates that the beam should be thin to reduce velocity spread and close to the circuit to reduce the power supply voltage for a given effective voltage. On the other hand, for a given cathode current density, the beam current is reduced for a thin beam, reducing power and gain. Appropriate tradeoffs are outlined in following sections.

2.4 FOCUSING

The geometry of the RBTWT requires a radial magnetic focusing field. Such a field can be provided by a pair of coaxial-cylindrical polepieces with a magnetomotive force maintained between them, either by coils or permanent magnets. In the center region of a long structure of this type, the flux lines would be purely radial, and the field intensity would vary as $1/r$. In a structure with a length-to-diameter ratio less than 1, excited by uniformly wound coils, the flux is purely radial only in the plane of symmetry, and varies less rapidly than $1/r$. Above or below the symmetry plane, the field has a component toward the plane.

A classical measure of the magnetic field strength needed to focus an electron beam is the so-called Brillouin field. Numerically, it is given by:

$$B_o = 1470 J_o^{1/2} V^{-1/4} \quad \text{(gauss)} \tag{2-15}$$

where:

J_o = current density in amperes/cm^2
V = effective beam voltage

For confined flow (cathode immersed in the magnetic field) the usual requirement for good focusing is a field strength equal to 1.8 to 2 times B_o.

Because of the radial expansion of the beam in the RBTWT, the magnetic field requirements are most severe at the cathode. Theoretically, to match the beam current density variation, the

field should vary about as $1/\sqrt{r}$. Actually, for a fixed circuit voltage, the effective beam voltage increases with increasing r, so the ideal field variation is a little more rapid than $1/\sqrt{r}$.

For small values of beam perveance, some form of PPM focusing may be possible. A system of ring-shaped polepieces with radially magnetized magnets between them could be used, or an alternating pattern of ring-shaped regions could be magnetized into a pair of disk magnets on either side of the tube. Applying the usual criteria for PPM-focused strip beams, the period of the magnetic field is found to be:

$$L_{max} = \frac{3.5\sqrt{V}}{B_o} \text{ (inches)} \qquad (2\text{-}16)$$

Since the usual radial-beam TWT would be designed for low voltage and high current (thus large B_o), PPM focusing appears impractical in most cases, since the useful field in the beam region would be very small for small values of the magnet period.

3.0 DESIGN PROCEDURES

All of the foregoing theoretical results, as modified by experimental measurements, can be combined to give a rough design procedure. A final design is usually best obtained with the aid of a computer. A flowchart for a computer program is given in Appendix D.

3.1 ASSUMPTIONS

What is usually required in a design procedure is a relationship between power output and gain, so that optimum tradeoffs can be made. To find such a relationship requires some basic assumptions about the tube performance.

The first of these assumptions is that the spiral circuit has a nominal upper frequency limit, which depends mainly on the outer radius, the dielectric substrate material, and the number of arms in the spiral. This limit is approached when the outer circumference of the spiral circuit equals n circumferential wavelenghts, where n is the number of arms in the spiral. (A circumferential wavelength is defined as the radial wavelength times cot ψ. The spiral angle ψ is defined in Figure 5.) The existence of this limit is postulated for several reasons, First, a spiral antenna is known to start radiating when the outer circumference is n wavelengths long. Even though a shielded circuit cannot radiate, some change in propagation characteristics would be expected. Secondly, the finite nature of the spiral arms would be expected to reduce the interaction impedance, since the radial electric field is partially short-circuited by the metallic conductors. This effect is particularly severe at the outer edge of the circuit. A quantitative analysis of this effect is given in Appendix C. Finally, experimental results indicate greatly reduced interaction above the "critical" frequency.

Numerically, this critical frequency is given by

$$f_c = \frac{v_p}{2\pi r_2 \tan \psi} \tag{3-1}$$

where v_p is the radial phase velocity. From Appendix A, v_p/c for a thick dielectric approaches $[2/(\epsilon' + 1)]^{1/2} \tan \psi$, where ϵ' is the relative dielectric constant of the substrate. So,

$$f_c \simeq \frac{2.66n}{r_2\sqrt{\epsilon' + 1}} \tag{3-2}$$

For thin shielded dielectrics or closely spaced circuits, the critical frequency is somewhat less than the value given by Eq. (3-2). For special geometries, as for example one with a gap between the substrate and the shield, the critical frequency might be somewhat higher than indicated by Eq. (3-2).

Another assumption which is necessary to arrive at a design procedure concerns the interaction impedance K. Appendix A and Figure 7 show that for dielectric thicknesses greater than about twice the circuit separation ($s/\ell > 4$), the theoretical impedance at the circuit is approximately:

$$K \simeq \frac{30}{kr} \cdot \frac{1}{\epsilon' + 1} \tag{3-3}$$

For an electron beam filling half the space between circuits, the reduction factor of Eq. (2-2) can be approximated by

$$F_1 = \frac{K_{av}}{K_{ckt}} \simeq \frac{1 + 0.1(\gamma\ell)^2}{\cosh^2(\gamma\ell)} \tag{3-4}$$

Combining this factor with the impedance reduction due to the finite width of the spiral arms (Appendix C) gives an overall impedance reduction factor of

$$\frac{K_{actual}}{K_{ideal}} = F_1 \cdot M = 2\,\frac{1 + 0.1(\gamma\ell)^2}{\cosh^2(\gamma\ell)} \left[\frac{\sin\left(\frac{\gamma w}{2}\right)}{\gamma w}\right]^2 \tag{3-5}$$

where w is the width of the spiral conductor and also the space between conductors. Since w varies with radius, M is a function of both frequency and radius. A plot of $F_1 \cdot M$ vs $\gamma\ell$ with w/ℓ as a parameter is shown in Figure 9.

To express F_1 and M in terms of convenient design parameters requires some assumptions relating $\gamma\ell$ to the beam and circuit parameters. Typically, the effective beam voltage is about 50% higher than the "cold" circuit velocity expressed as a voltage, due to space charge effects. Also, the beam can be assumed to fill approximately half the space between circuits, so $t = \ell$. Thus,

$$\gamma\ell \simeq \frac{2\pi f t}{v_p} = 330\,\frac{ft}{\sqrt{V_o}} \tag{3-6}$$

Eliminating t by use of Eq. (2-10),

$$\gamma\ell \simeq 129 f S_1^{1/2} V_o^{1/4} (J_o r_c/r_1)^{-1/2} \tag{3-7}$$

For equal conductor and space widths, $w = \pi r \tan\psi/n$, where n is the number of arms in the spiral. Thus, for thick dielectrics,

$$\gamma w \simeq \frac{1.2 f r}{n}\sqrt{\epsilon' + 1} = \pi\left(\frac{r}{r_2}\right)\left(\frac{f}{f_c}\right) \tag{3-8}$$

where f_c is the "critical" frequency given by Eq. (3-1), so:

$$F_1 = \frac{\left(1 + 1664\,\frac{f^2 S_1 \sqrt{V_o}}{J_o r_c/r_1}\right)}{\cosh^2\left[129 f S_1^{1/2} V_o^{1/4} (J_o r_c/r_1)^{-1/2}\right]} \tag{3-9}$$

$$M = \frac{2r_2^2 f_c \left(\frac{\pi r f}{2r_2 f_c}\right)}{(\pi r f)^2} \tag{3-10}$$

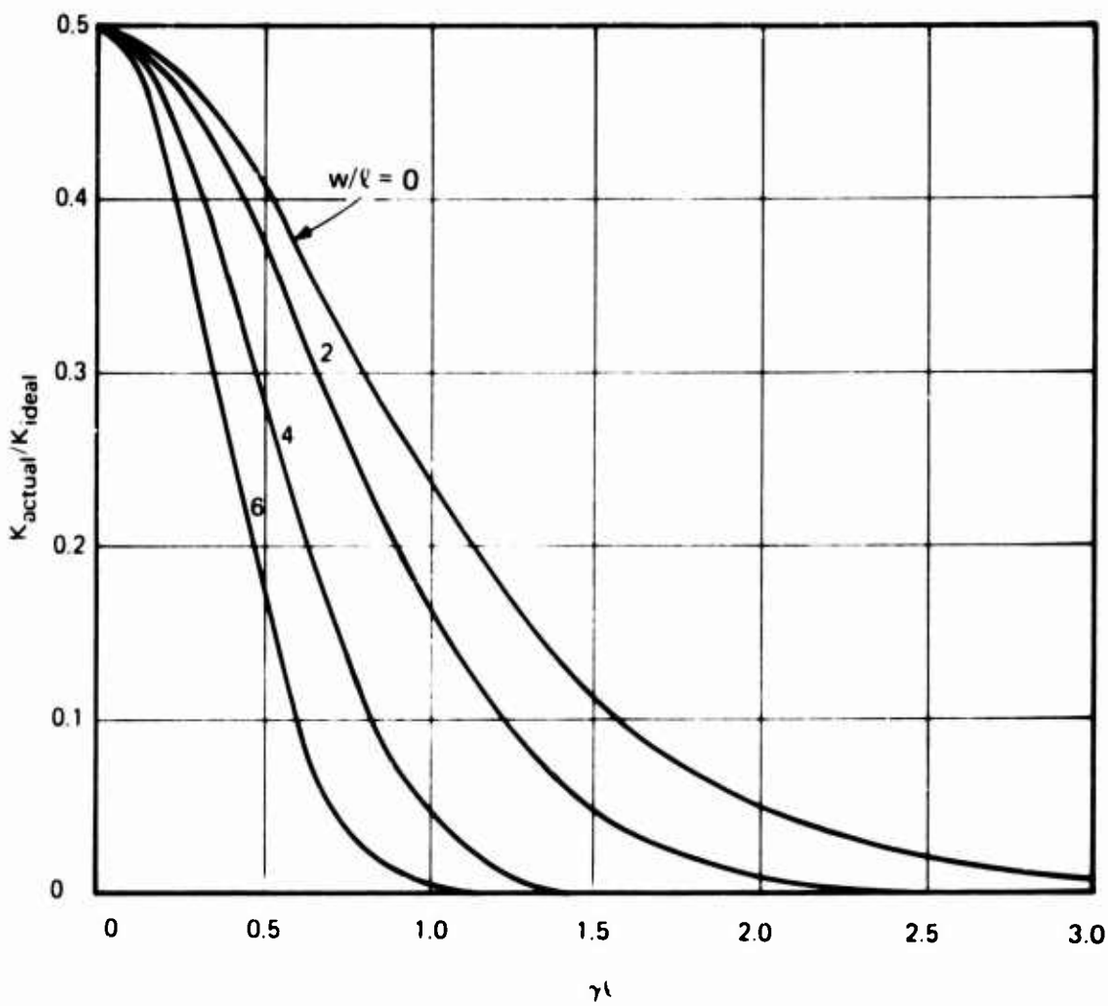

TP A-9531

Figure 9. Overall Impedance Reduction Factor

Since M appears only to the one-third power, it is convenient to approximate it by

$$M^{1/3} \simeq 0.8 - 0.2\left(\frac{rf}{r_2 f_c}\right)^2 \tag{3-11}$$

The estimated power output of Eq. (2-9) then becomes:

$$P_{out} = 2\left[\frac{K_2}{4}\right]^{1/3} I_o^{4/3} V_o^{2/3} \tag{3-12}$$

Here, K_2 is the actual interaction impedance at the outer edge of the circuit.

$$K_2 = \frac{56\alpha}{f r_1(\epsilon' + 1)} F_1 M_2 \tag{3-13}$$

where:

α = ratio of inner to outer circuit radius
M_2 = value of M at the outer radius
r_1 = inner radius (inches)
f = frequency (GHz)

For cathode current density in A/cm^2 and dimensions in inches,

$$I_o = 40.54 J_o r_c t \tag{3-14}$$

Eliminating t by use of Eq. (2-10) gives:

$$I_o = 15.96 J_o^{1/2}\left(\frac{r_c}{r_1}\right)^{1/2} S^{1/2} V_o^{3/4} r_1 \tag{3-15}$$

Substitution into Eq. (3-12) gives:

$$P_{out} = 193\left[\frac{F_1 M_2}{f(\epsilon' + 1)}\right]^{1/3} \alpha^{4/3} r_2 (S J_o r_2 / r_1)^{2/3} V_o^{5/3} \tag{3-16}$$

The "one-wave" gain of Eq. (2-7) can also be written in terms of the above parameters. If β_e is considered constant (actually it varies due to the radial expansion of the beam), and if C at a given frequency is considered to be the "ideal" value reduced by the average of the factor $M^{1/3}$ over the interval r_1 to r_2, then

$$G_{(one\text{-}wave)} \sim \frac{6.9(2\pi f) C F_2 \bar{\chi}(r_2 - r_1)}{U_o} - 10 \log \alpha \tag{3-17}$$

where:

$\bar{\chi}$ = average value of the growing wave gain parameter χ_i (Appendix B)

U_o = average dc beam velocity = $0.0233\sqrt{V_o}$ in/ns

and F_2 is given by

$$F_2 = 1 - \frac{f^2}{12 f_c^2}\,(1 + \alpha + \alpha^2) \tag{3-18}$$

Extensive calculations indicate that a reasonable choice of $\bar{\chi}$ for rough designs is about 0.5, typically varying from perhaps 0.7 to 0.4 from the low to the high end of an octave band. Thus:

$$G \simeq \frac{5640 F_1^{1/3} F_2 f^{2/3} r_2 (1-\alpha)(S J_o r_c/r_1)^{1/6}}{(\epsilon' + 1)^{1/3} V_o^{7/12}} - 10 \log \alpha \tag{3-19}$$

Equations (3-16) and (3-19) can be solved simultaneously as a function of the various parameters. Obviously, current density and perveance per square should be as high as possible to maximize both power and gain. Voltage, however, should be large for maximum power but small for maximum gain. The same is true for α. In choosing a design, it must be kept in mind that the overall net gain will be less than that given by Eq. (3-19) by the amount of the launching loss. A typical value of launching loss might be 10 dB. In addition, at saturation drive levels, a gain reduction of about 5 dB can be expected due to nonlinear compression effects.

Figure 10 shows a plot of possible designs at f = 1 GHz, $S = 7 \times 10^{-6}$, J_o = 6 A/cm^2, $r_c/r_1 = 0.9$, $\epsilon' = 6.6$, r_2 = 1.7 in., f_c = 1.13 GHz. The parameters are V_o and α. Suitable tentative designs can be chosen from such plots, and detailed performance can than be calculated by computer.

3.2 FREQUENCY SCALING

In terms of the size of the rf circuit, the existence of a "critical" frequency dictates that the maximum circuit diameter be proportional to the design wavelength. In the following discussions, the product $f \cdot r_2$ is considered to be a constant, as well as the value α.

At low frequencies, the limiting factor in designing a radial-beam TWT is usually perveance per square, assuming current density is fixed at the maximum practical value. Under these conditions, the maximum output power for fixed gain varies as $f^{-16/7}$. It is necessary to vary the operating voltage as $f^{-4/7}$ as the design frequency is changed in order to keep the gain constant.

At high frequencies, the limiting factor becomes the separation between circuits, since the rf field variation across the beam becomes significant. This effect appears in the power and gain expressions as the factor F_1. If F_1 is to remain constant as frequency is increased, the factor $S\sqrt{V_o}/(J_o r_c/r_1)$ must decrease as the square of the frequency. Since J_o is usually fixed at the largest possible value, and r_c/r_1 is normally nearly unity, the product $S\sqrt{V_o}$ must vary as f^{-2}. Under these conditions, the gain will remain constant only if S varies as $f^{-3/2}$ and V_o varies as $1/f$, resulting in an output power variation as f^{-4}. Because of the rapid decrease in power with increasing frequency, power density is usually not a limitation.

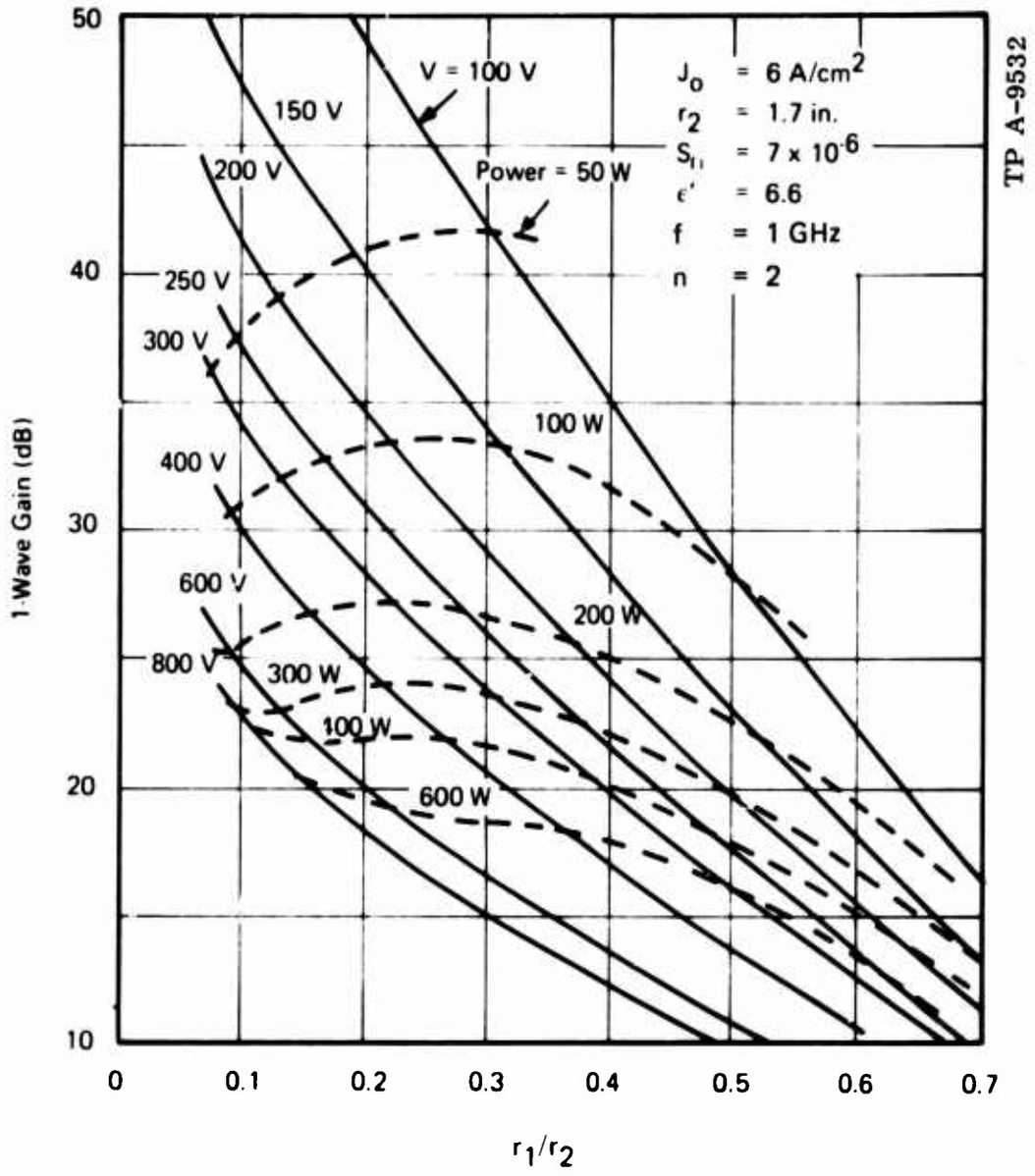

Figure 10. L-Band Design Plot

In intermediate frequency ranges, the slope of the power vs. frequency curve varies between the two extremes outlined above. Figure 11 shows a composite plot based on $n = 2$, current densities of 6 and 12 A/cm^2, using BeO substrates, and an assumed one-wave gain of 25 dB. In the low-frequency range, the perveance per square is taken to be 7×10^{-6} maximum, while in the upper range it is chosen to maximize power output at fixed gain.

3.3 TUBE DESIGN

At the time that the presently built tubes were designed, it had not been determined that the impedance reduction due to the finite nature of the spiral arms was as severe as indicated by Eq. (3-10). Consequently, the factor M in Eq. (3-16) was taken to be unity, and the factor F_1 in Eqs. (3-16) and (3-19) was taken to be 0.8. The factor F_2 in Eq. (3-19) was also taken to be unity.

Two different designs were used in the present program. Both used BeO substrates to take advantage of the relatively low dielectric constant and good thermal properties of this material. Both employed two arms per spiral. In the first design, a cathode current density of 6 A/cm^2 was chosen as being a practical upper limit for a directly heated dispenser-type cathode. Focusing fields are also acceptable at this current density. In the second design, a current density of 2 A/cm^2 was used in order to overcome focusing difficulties encountered in the first tube. The final design parameters for both designs are shown in Table I.

Table I

Comparison of Final Design Parameters for Desigrs I and II

Parameters	Design I	Design II
Frequency (GHz)	0.5 – 1.0	0.5 – 1.0
Supply voltage (V)	300	300
Beam current (A)	4.0	3.1
Cathode diameter (in.)	1.2	1.8
J_o (A/cm^2)	6.0	2.0
Beam thickness (in.)	0.025	0.040
Circuit separation (in.)	0.050	0.070
Spiral constant	0.042	0.05
Inner circuit diameter (in.)	1.36	2.0
Outer circuit diameter (in.)	3.4	4.0
Dielectric thickness (in.)	0.150	0.150
f_c (MHz)	1.04*	0.88*
Modulating electrode	nonintercepting	gridded

* *Values are based on theoretical phase velocities. Actual velocities were somewhat higher.*

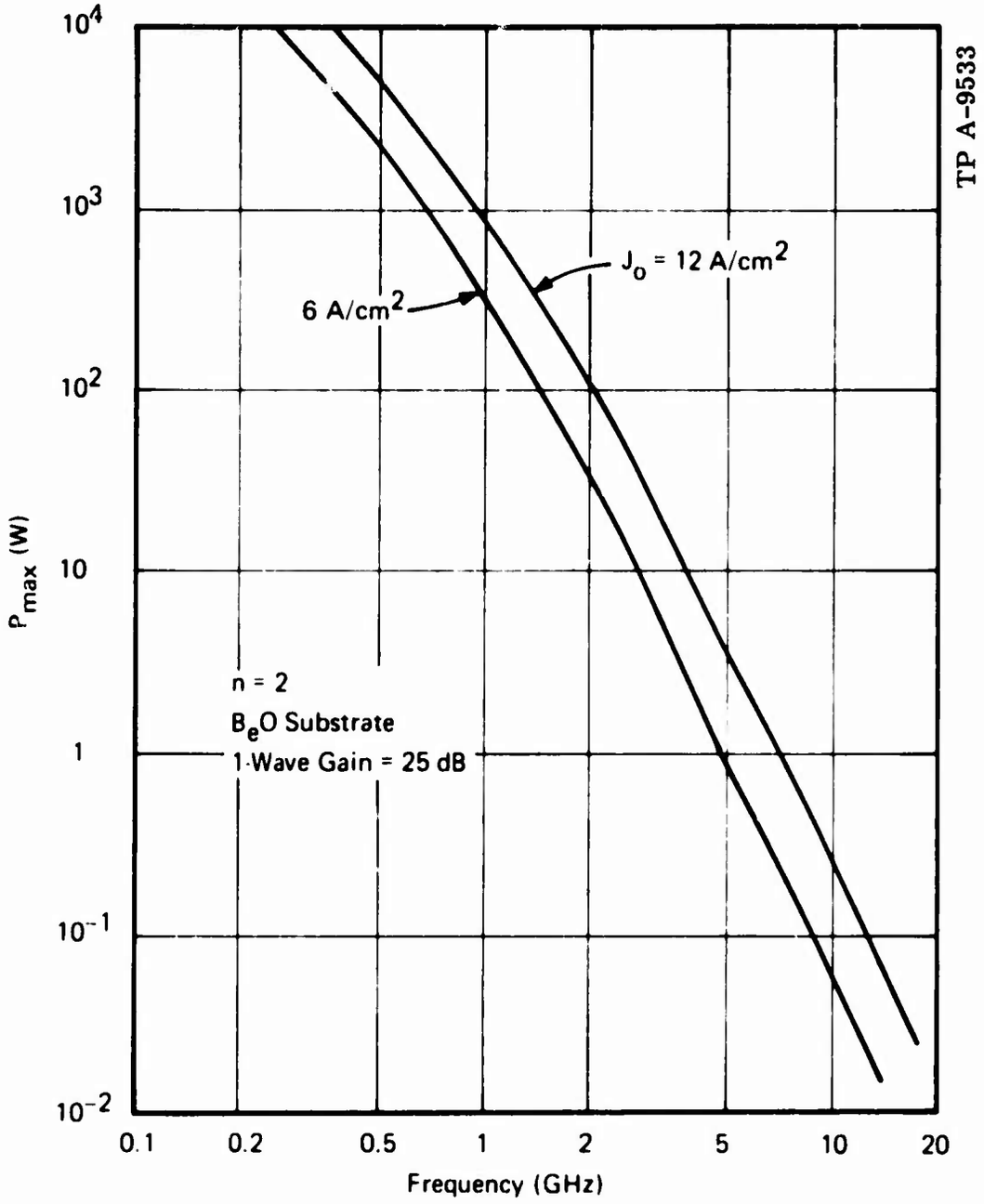

Figure 11. Maximum Output Power vs Frequency

The spiral constant, or pitch angle of the spiral arms, was determined with the aid of a computer, using the relationships of Appendix A. As a rough approximation, the radial velocity of the circuit wave, expressed as a voltage, is given by:

$$V_s = \frac{512072a^2}{(\epsilon' + 1)} \tag{3-20}$$

where a is the spiral constant ($a = 1/\cot \psi$). A more precise determination can be obtained from a plot such as Figure 6.

For proper operation, the value of V_s as given in Eq. (3-20) should be equal to or somewhat less than the equivalent voltage of the slow space-charge wave in the beam, which in turn is less than the effective beam voltage. Since the space-charge parameters of the beam vary with radius, synchronization cannot be maintained over the entire radial distance. In addition, the launching loss A varies with the ratio of circuit-to-electron velocity. For maintaining gain flatness across an octave band, typical calculations indicate that the effective beam voltage may be as much as 1.5 times the value of V_s. In addition, the supply voltage must be higher than the effective voltage by an amount given by Eq. (2-14).

3.4 ELECTRON GUN DESIGN

As a first approximation, the electron gun can be designed on the basis of strip-beam parameters. In a nongridded gun, the cathode-anode spacing should probably not be less than the anode aperture dimension in order to avoid detrimental lens effects. A check of the cathode-circuit geometry shows that for this condition at P_{out} = 300 watts, the cathode current density would be much too low. Therefore, an intermediate anode must be placed between the cathode and the circuit, operating at a voltage higher than the circuit. A simple "diode" calculation indicates that for design I, an anode voltage of about 700 volts would be required.

Details of focus electrode geometry and anode placement were worked out using a computer program to plot electron trajectories. A typical plot for design I is shown in Figure 12(a). As can be seen, the gun has strong lens effects, as indicated by the large beam ripple, but these apparently cannot be avoided without departing from the flat "printed-circuit" form of gun electrodes.

For design II, it was decided to use a mesh grid, both to avoid lens effects, and to operate at lower voltages. As an approximation to the grid, a single element was inserted between the cathode and circuit, and the resulting trajectories calculated. The results are shown in Figure 12(b). The reduction in beam ripple is apparent, due mostly to the reduced current density.

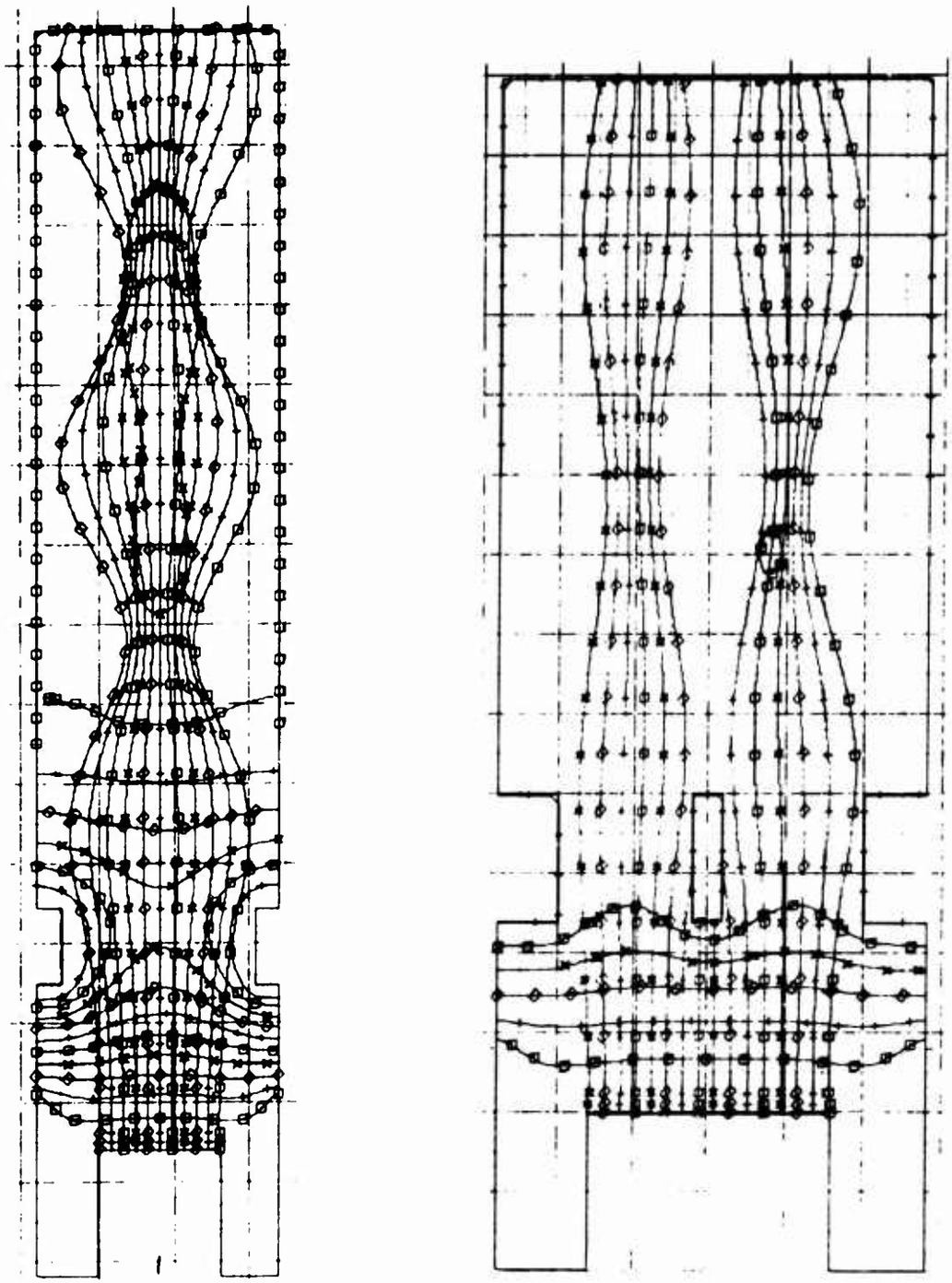

(a) (b)

Figure 12. Calculated Trajectories for Radial Beams

4.0 EXPERIMENTAL RESULTS

Two tubes (serial numbers 2 and 3) were built to design I specifications, and one (serial number 4) to design II. Experimental results are presented in the following sections.

4.1 RF MATCHES

The RBTWT was constructed as an eight-port device with four separate circuits. Only one propagating mode is desired, that for which the fields of all circuits are in phase at a given radius. To satisfy this condition, the input ends of all four spirals must be driven in phase. A conventional 50 Ω matched power divider was used to divide the input power equally between the two halves of the tube. For design I, the impedance at the inner ends of the individual spiral arms was not 50 Ω, so a strip-line power divider was devised, which also provided some impedance transformatio. ... Figure 2). Three conventional 50 Ω matched power combiners were used to combine the signals from the four output ports. For design II, all impedances were reasonably close to 50 Ω, so conventional power dividers were used throughout. Typical rf match data are shown in Figure 13. Since the individual matches of each side of the circuit (curve C) were generally under 2:1 vswr, the much higher vswr obtained when the two sides were combined suggests some difference in phase velocity between the two sides, particularly in the upper half of the band for tube 2.

4.2 INSERTION LOSS

The insertion loss of the spiral circuits can be estimated on the basis of strip-line theory, taking into account the constantly changing width of the line. For the present designs, this kind of estimate predicts a loss of 0.35 to 0.5 dB over the 0.5 to 1 GHz band. Measured data is shown in Figure 14. The difference, particularly for tubes 2 and 3, is thought to be due to the relatively poor quality of the copper plating on the spiral lines. The large variations in insertion loss above 800 MHz for tubes 2 and 3 are due to the poor rf matches.

For tube 4 (design II) there are several relatively sharp "holes" in the cold transmission. The reason for these is not obvious, although the one near 9 GHz can be shifted in frequency by changing the lengths of the coaxial sections between the tube and the input power dividers. The one at 8 GHz cannot be influenced externally, and in addition has some peculiar properties, as noted below.

4.3 GAIN

Gain measurements were made on all three tubes, but problems connected with focusing and/or oscillations prevented testing them at more than a fraction of the design beam current. Oscillation frequencies were in the 200 to 400 MHz range, and appeared to be associated with a "transverse" mode, i.e., one in which electric fields lines go across from one circuit to the other. The theory presented in Appendix A indicates that such modes have phase velocities only slightly higher than those of the desired mode, and thus could interact with the beam. The fact that the beam transmission decreased markedly when oscillations were present, but not under "normal" high rf drive levels, indicates the presence of strong transverse fields. The starting currents for these oscillations increased greatly when each port of the tube was individually terminated, indicating that perhaps a low frequency resonance in the transverse mode was established by connecting the two sides of the circuit together. Certainly, the power dividers used would be equivalent to a short circuit for an antisymmetric mode.

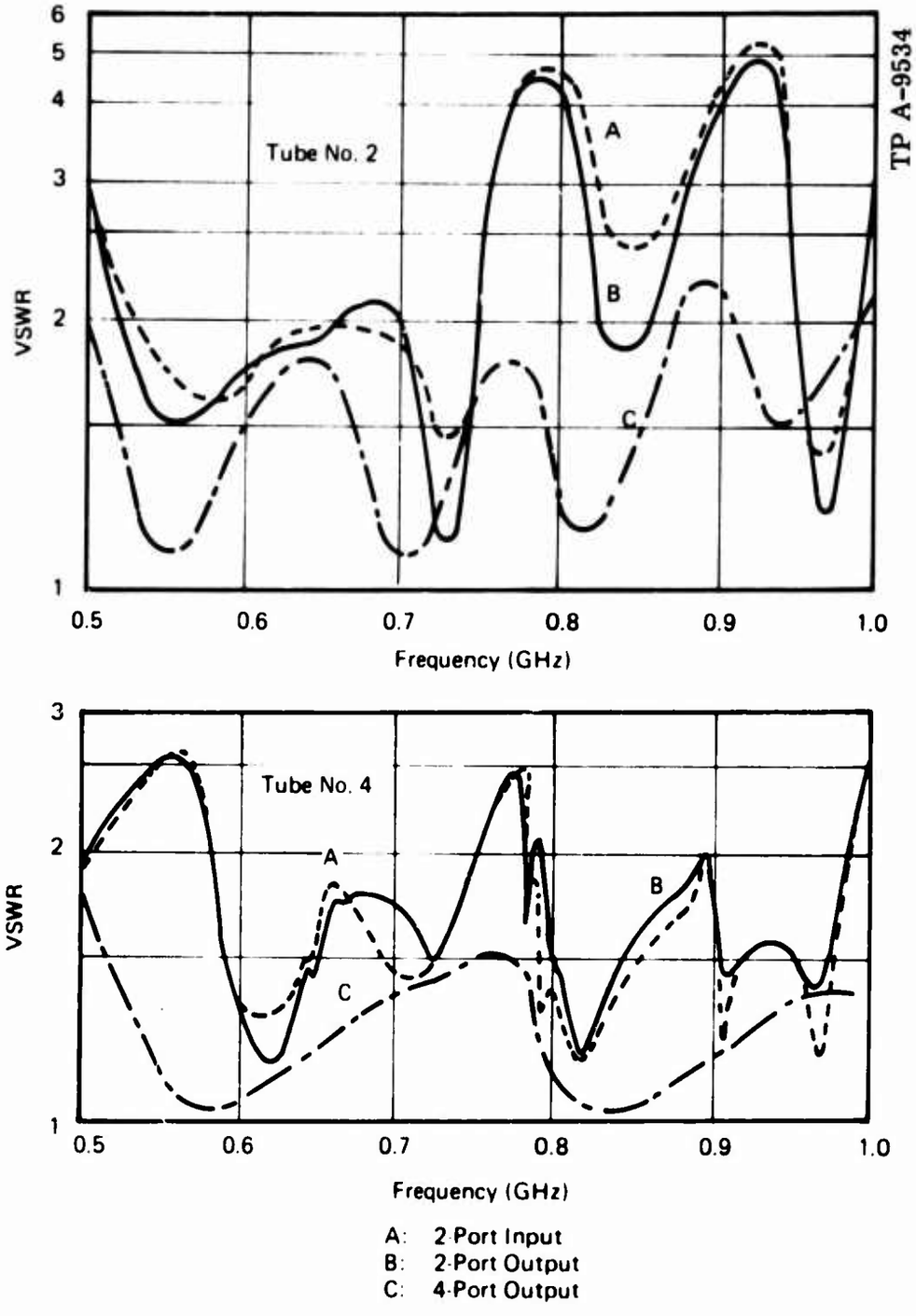

Figure 13. Rf Matches for Spiral Circuits

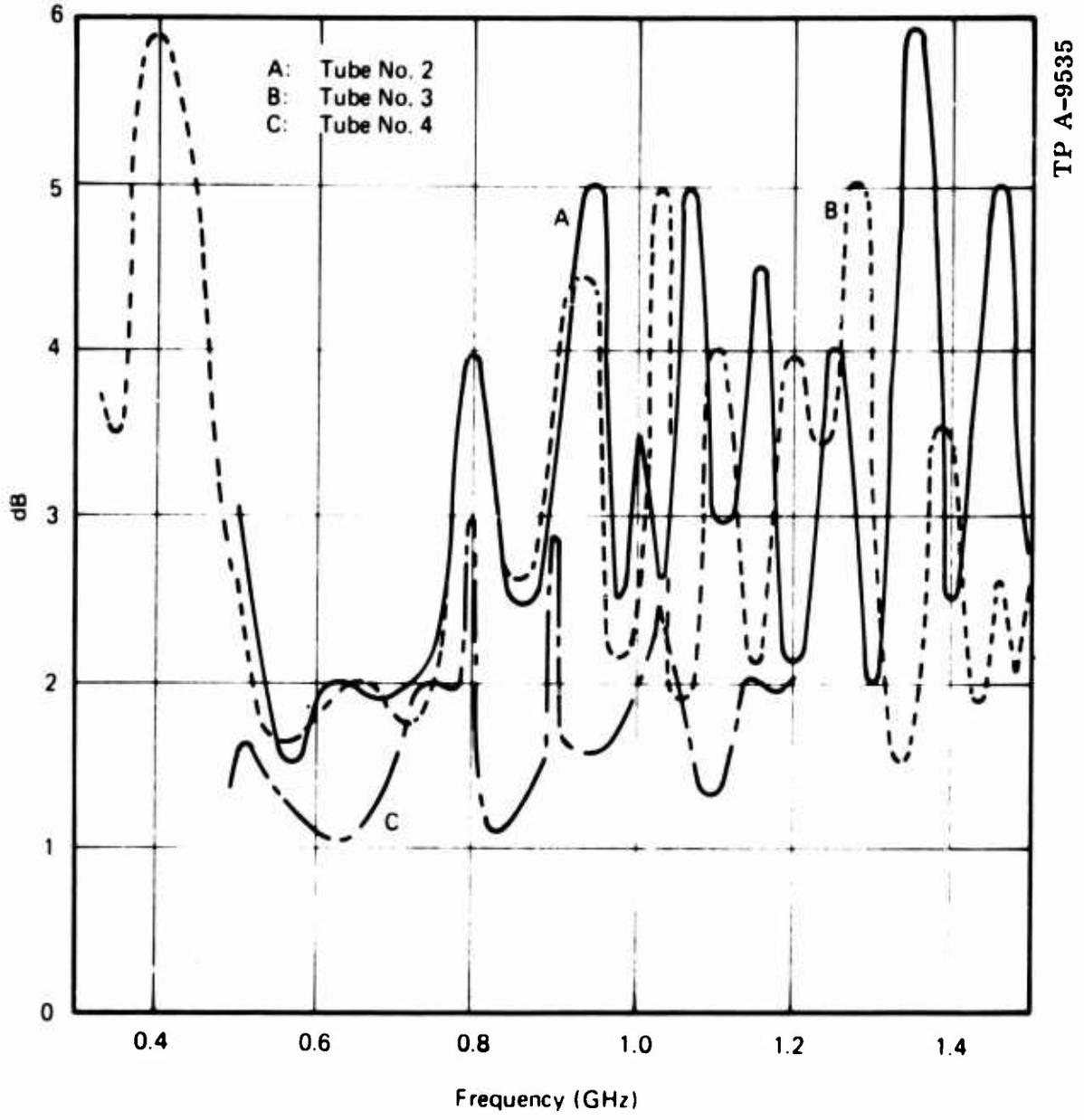

Figure 14. Insertion Loss of Spiral Circuits

In addition to oscillation problems, tubes 2 and 3 exhibited a beam instability which was presumably due to charging of exposed ceramic surfaces by the electron beam.[3] This charging was characterized by hysteresis effects, being dependent on tube temperature, focusing field strength, beam current, the direction in which the beam voltage was changed, and whether or not the tube was oscillating. Usually, oscillation and charging occurred together, one serving to trigger the other, but under certain conditions it was possible to observe them separately.

Tube 4 did not exhibit any obvious charging. It did oscillate however, at collector currents above 0.55 A. In addition, the grid interception was abnormally high. Initially the interception at low currents was about 16%, which corresponds closely to the grid transparency. As the tube was operated over a period of hours, the interception rose to about 30%. At higher currents, the interception was even greater, being 65% at a cathode current of 3 A. The first effect may be due to the gradual plugging of the grid holes with evaporated cathode material, but the explanation for the latter effect is not known.

All tubes were focused in a radial magnetic field provided by a pair of opposing "pancake" coils in a cylindrical-coaxial magnetic yoke (see Figure 2). The space between coils was 2 in., and the outside diameter was 8 in. The radial field strength varied from about 2400 gauss at a radius of 0.5 in. to about 1000 gauss at a radius of 2.0 in. Beam transmission beyond the anode or grid was greater than 90% for all tubes, when not oscillating.

The gain added by the beam, or "electronic" gain is shown in Figure 15 for tubes 3 and 4. Results for tube 2 were almost identical with those for tube 3. The net gains of the tubes can be obtained by subtracting the insertion loss shown in Figure 14. Agreement with theoretical values is only fair. It could of course be improved by assuming a different form of impedance reduction factor.

The sharp spike in insertion loss for tube 4 at about 800 MHz was found to correspond to a region of little or no electronic gain for normal beam voltages. Some gain could be obtained for much lower voltage, indicating perhaps that most of the energy at this frequency is being carried in a mode with a much lower phase velocity than that of the normal mode. The region around 900 MHz did not show such an effect, although it too had a sharp spike in the insertion loss. No such frequency regions were noted in tubes 2 and 3.

Figure 16 shows the measured circuit velocity as determined from the beam voltage for "zero" interaction at small currents. Theoretical values are shown for comparison.

The power required to heat the cathode was about 30 W for tubes 2 and 3, and about 45 W for tube 4.

4.4 POWER

Tube 3 was tested for power output at several frequencies. A driver with about 16 W output at 580 MHz was available, so that with the beam off, the tube output was about 10 W. (Insertion loss = 2 dB.) With a collector current of 0.28 A (pulsed, 1% duty) and a circuit voltage of 210 V, the peak output power varied from 16 W to 30 W, depending on the magnetic field strength. (The higher output was obtained with reduced magnetic field.) Since the tube was undoubtedly oscillating at this current, the significance of the measurement is uncertain, although oscillation power with the drive removed appeared to be less than 0.5 W.

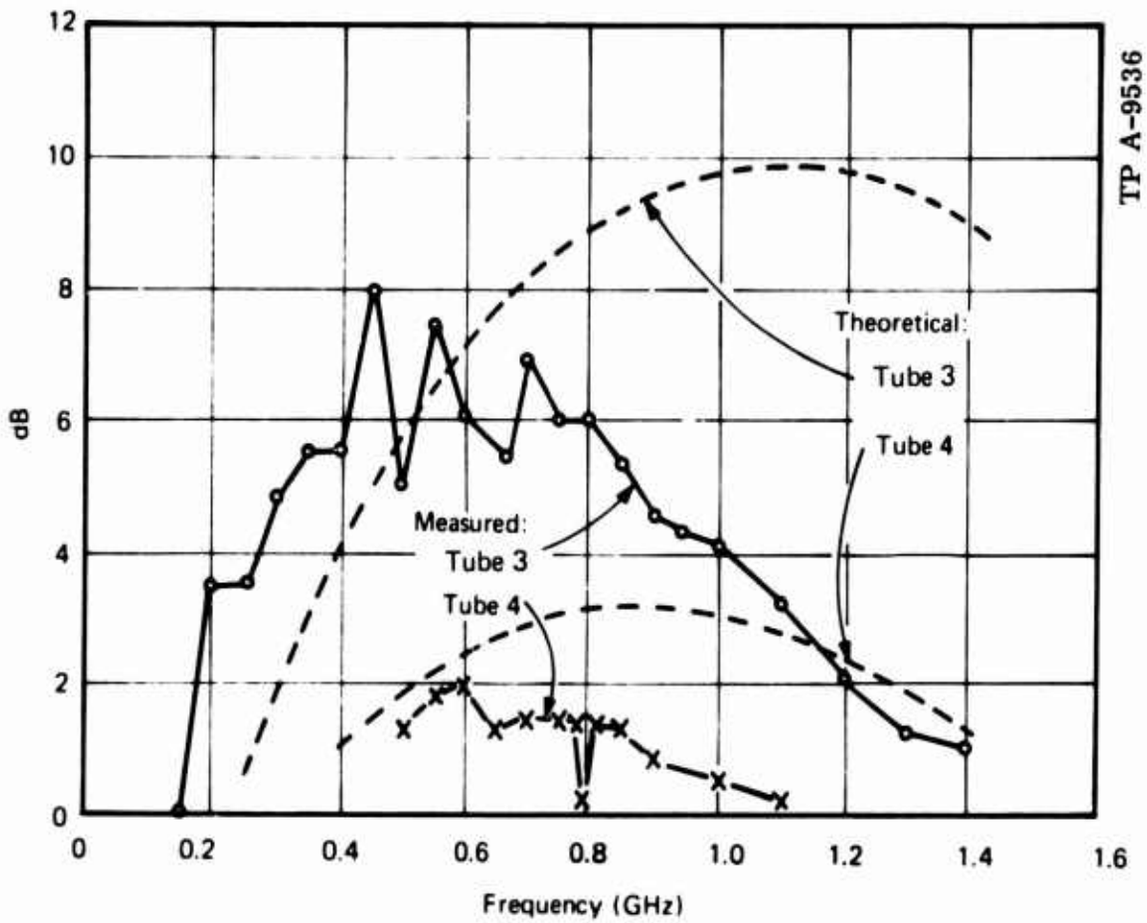

Figure 15. Electronic Gain of RBTWT No. 3 and No. 4

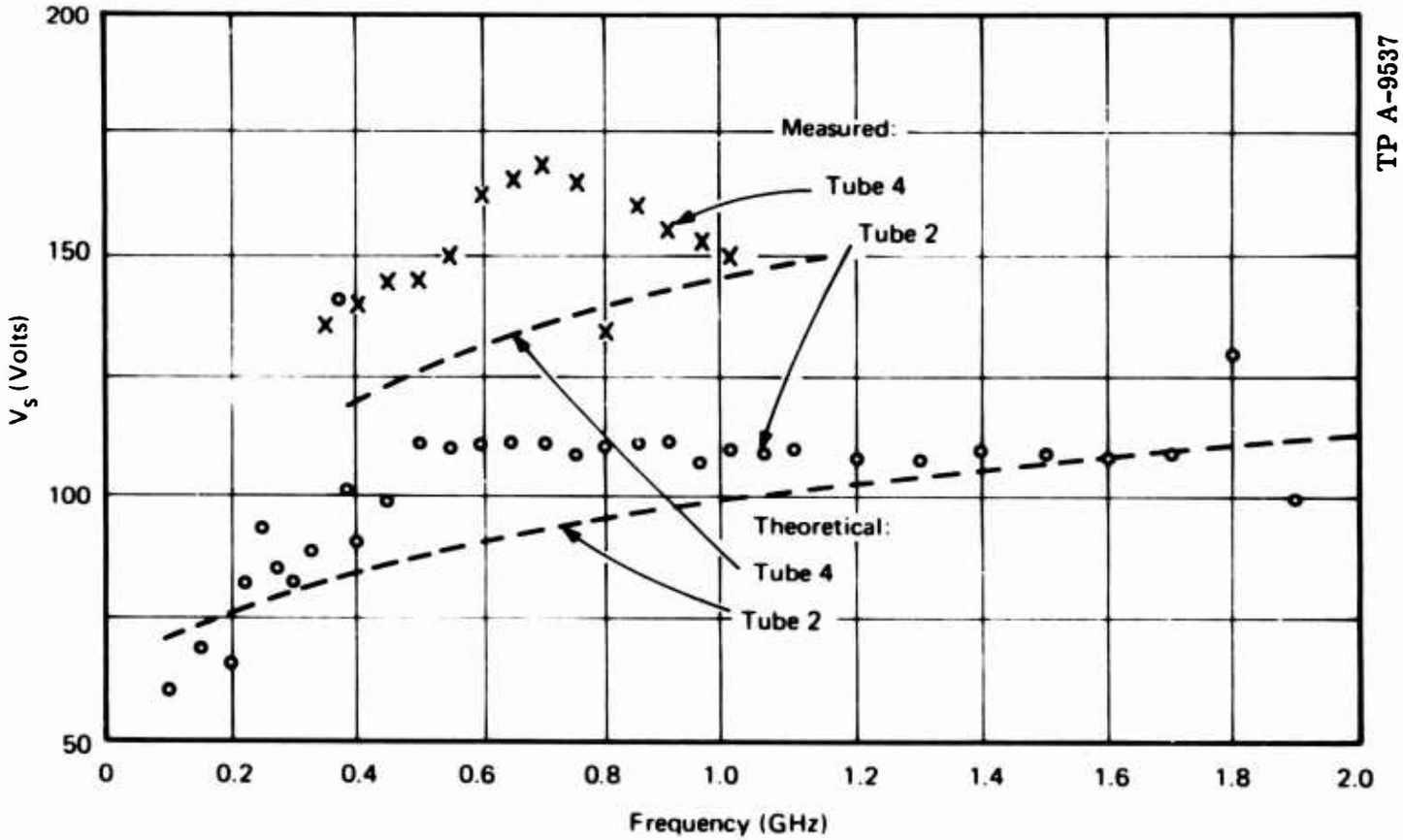

Figure 16. Circuit Velocity of RBTWT No. 2 and No. 4

Under similar conditions at 950 MHz, the output power increased from 7.5 W with no beam to 11 W with the beam on.

In another measurement, tube 3 was run cw at a cathode current of 0.2 A (the limit of the able supply) with an output power of 15 W. No undue heating effects were observed.

Power tests were not made on tube 4 because of its low gain.

5.0 CONCLUSIONS AND RECOMMENDATIONS

The radial beam TWT appears to give relatively flat gain over an octave bandwidth, with promising power capabilities at low frequencies. Performance is generally in accord with theory, considering the unknown effects of the discrete nature of the spiral arms, and the uncertainties in the beam shape and distribution. The principal lack of agreement between theory and measurement is the rapid falloff in measured gain as the "critical" frequency is approached, indicating a more severe reduction in interaction impedance than has been assumed.

Suppression of internal oscillations appears to be a serious problem. Some type of selective interaction may be required to prevent high fields from existing in unwanted modes.

Considerable improvement in performance can be gained by raising the impedance of the spiral circuit, principally by decreasing the dielectric loading. The dielectric loading can be reduced by removing some of the dielectric between spiral arms, in effect supporting the circuit on spiral ridges, or by using a thin dielectric substrate with a gap between the substrate and the ground plane. In the latter case, the problem of transferring heat across the gap would have to be solved. Reference to design Eqs. (3-2), (3-12), and (3-15) indicates that, for a fixed gain, the maximum power output at any frequency is proportional to $(\epsilon' + 1)^{-3.21}$ where ϵ' is the effective relative dielectric constant of the substrate. Thus, reducing ϵ' from 6.6 (for BeO) to 3.3 by means of a gap or dielectric shaping will increase the power by a factor of 6.2. Conversely, for a fixed power, the gain would be increased by a factor of about 1.5 to 2, depending on the gain and the particular value of r_2/r_1 being employed. Also, further improvement in tube performance can be gained by utilizing a spiral slow wave circuit with more than two spiral arms.

6.0 LITERATURE CITED

[1] J. R. Pierce, "Traveling Wave Tubes," Van Nostrand, New York, 1950.

[2] D. A. Dunn, "Traveling Wave Amplifiers and Backward Wave Oscillators for UHF," *IRE Trans.* Vol. ED-4, pp. 253-255, July 1957.

[3] For a description of similar behavior in a helix TWT, see Maurer *et al.*, *IEEE Trans. on Elec. Dev.*, ED-12, No. 1, p. 40.

[4] V. S. Savel'yev, "Interaction of a Radially Diverging Electron Stream and a Radially Traveling Electromagnetic Wave," *Rad. Eng. and Elect. Phys.*, Vol. 12, No. 6, pp. 941-947, 1967 (English translation).

[5] J. C. Slater, "Microwave Electronics," Van Nostrand, New York, 1950, Chapter 8.

[6] P. K. Tien, "Traveling-Wave Tube Helix Impedance," *Proc. IRE*, Vol. 41, Nov. 1953, p. 1617.

7.0 GLOSSARY

a, b, c, d	boundary values (Appendix A)
A, B, C, D	coefficients in Maxwell's equations (Appendix A)
a	spiral constant = $1/\cot \psi$
b	velocity parameter (Eq. B-4)
B_o	"Brillouin" focusing field (Eq. 2-15)
C	Pierce gain parameter (Eq. 2-5)
d	loss parameter (Eq. B-4)
E_n	components of initial field (Eq. B-10)
E_T	total initial field
f	frequency (GHz)
f_c	"critical" frequency (Eq. 3-1)
F_1	impedance reduction factor (Eq. 3-4)
F_2	impedance reduction factor (Eq. 3-14)
I_o	beam current (amperes)
j	$\sqrt{-1}$
J_o	beam current density (A/cm^2)
k	propagation constant = $\omega^2 \mu \epsilon_o$
K	interaction impedance (Eq. A-19)
ℓ	midplane to circuit spacing
M	impedance reduction factor (Eq. 3-10)
m	fractional velocity spread (Eq. 2-11)
n	number of arms per spiral
p	plasma frequency reduction factor
P	rf power flowing radially
r_c	cathode radius
$r_{1,2}$	inner and outer circuit radius, respectively
R	Hankel function (Eq. A-3)
t	beam thickness
T	space-charge parameter (Eq. B-5)
U_o	dc beam velocity (Eq. 22)

v_p	phase velocity of circuit
V_o	effective dc beam voltage = $\bar{V}$
V_{ckt}	dc voltage between cathode and circuit
V_e	beam-edge dc voltage
V_s	equivalent voltage of radial phase velocity
X	normalized propagation constant (Eq. A-8)
α	ratio of circuit radii = r_1/r_2
β	axial propagation constant
β_e	beam propagation constant = ω/u_o
γ	radial propagation constant
Γ	combined propagation constant
Γ_1	circuit propagation constant
δ_n	incremental propagation constant
ϵ_o	free space permitivity = 8.842×10^{-12} F/m
ϵ'	relative dielectric constant of substrate
η	normalized impedance = 377 Ω
μ	free space permeability = $4\pi\times10^{-7}$ H/m
ψ	spiral pitch angle
ω	angular frequency = $2\pi f$

APPENDIX A

SPIRAL CIRCUIT THEORY

Solutions of Maxwell's equations in cylindrically symmetrical systems involving waves traveling radially outward are most conveniently expressed in terms of Hankel functions and hyperbolic functions. A useful form for non-θ-varying radial components of E or H is (with the factor $e^{j\omega t}$ understood):

$$W_r = H_1^{(2)}(\gamma r)\,[A\cosh(\beta z) + B\sinh(\beta z)] \tag{A-1}$$

where $H_1^{(2)}(\gamma r)$ is the Hankel function of the second kind and order 1. β and γ are the axial and radial propagation constants, respectively. The relationship between β and γ is given by:

$$\beta^2 = \gamma^2 + \omega^2\mu\epsilon$$

so that for slow waves, $\beta \simeq \gamma$. For convenience, the asymptotic expansions of the Hankel functions will be used, since for slow waves and practical circuits, the minimum value of γr will be usually much greater than unity. Let

$$R = \sqrt{\frac{2}{\pi\gamma r}}\; e^{-j(\gamma r - 3\pi/4)} \tag{A-2}$$

for $\gamma r \gg 1$,

$$H_1^{(2)}(\gamma r) = R \quad , \quad H_o^{(2)}(\gamma r) = R\,e^{-j\pi/2} = -jR \tag{A-3}$$

The dimensional notation to be used is shown in Figure A-1. Due to the symmetry about the midplane, field expressions are needed only for the regions shown. Using the notation of Eq. (A-3) and assuming that $\gamma = \beta$, the field components are (with a factor of $e^{j(\omega t - \gamma r)}$ understood):

In the space between the circuits:

$$E_r = R[A_1\cosh(\gamma z) + B_1\sinh(\gamma z)]$$

$$H_r = R[C_1\cosh(\gamma z) + D_1\sinh(\gamma z)]$$

$$E_z = jR[A_1\sinh(\gamma z) + B_1\cosh(\gamma z)]$$

$$H_z = jR[C_1\sinh(\gamma z) + D_1\cosh(\gamma z)]$$

$$E_\theta = \frac{j\omega\mu R}{\gamma}[C_1\sinh(\gamma z) + D_1\cosh(\gamma z)]$$

$$H_\theta = -\left(\frac{j\omega\epsilon_o R}{\gamma}\right)[A_1\sinh(\gamma z) + B_1\cosh(\gamma z)] \tag{A-4}$$

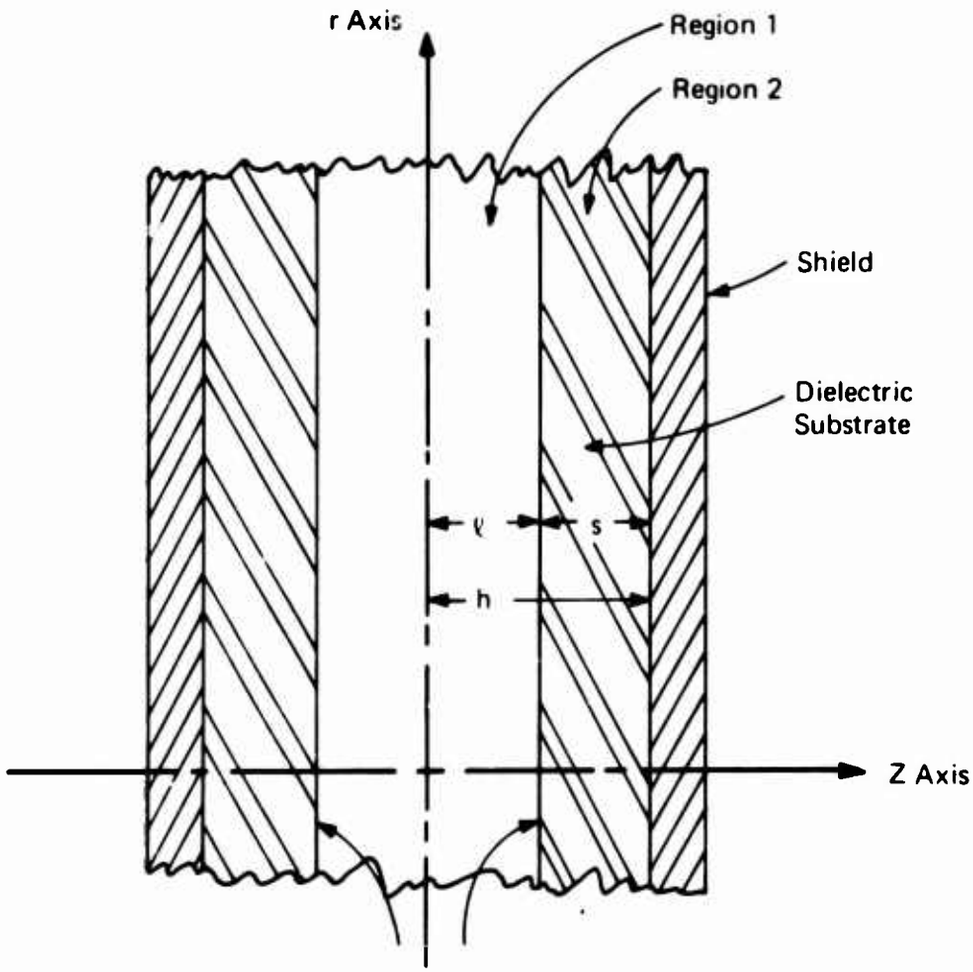

ψ = Constant

ψ is the angle between the normal to the radius and the conducting direction.

Figure A-1. Spiral Circuit Configuration and Notation

In the substrate:

$$E_r = RA_2 \sinh [\gamma(z-h)]$$

$$H_r = RC_2 \cosh [\gamma(z-h)]$$

$$E_z = jRA_2 \cosh [\gamma(z-h)]$$

$$H_z = jRC_2 \sinh [\gamma(z-h)]$$

$$E_\phi = \frac{j\omega\mu R}{\gamma} C_2 \sinh [\gamma(z-h)]$$

$$H_\theta = -\left(\frac{j\omega\epsilon_o\epsilon' R}{\gamma}\right) A_2 \cosh [\gamma(z-h)] \qquad \text{(A-5)}$$

The form of Eq. (A-5) was chosen to satisfy the boundary conditions at the shield. ϵ' is the relative dielectric constant of the substrate.

A1. DISPERSION

The boundary conditions at the circuit are the usual ones for an anisotropically conducting sheet:

$$E_{\theta 1} + E_{r_1} \tan \psi = 0$$

$$E_{r_1} = E_{r2}$$

$$E_{\theta 1} = E_{\theta 2}$$

$$H_{\theta 1} + H_{r_1} \tan \psi = H_{\theta 2} + H_{r2} \tan \psi \qquad \text{(A-6)}$$

where ψ is the angle between the perpendicular to the radial direction and the direction of conduction of the spiral sheet. For a logarithmic spiral, ψ is a constant.

Substituting for the field components gives the following set of equations:

$$j\eta X(C_1 b + D_1 a) + (A_1 a + B_1 b) = 0$$

$$A_1 a + B_1 b + A_2 c = 0$$

$$C_1 b + D_1 a + C_2 c = 0$$

$$-\frac{jX}{\eta}(A_1 b + B_1 a) + (C_1 a + D_1 b) + \frac{jX\epsilon'}{\eta} A_2 d - C_2 d = 0 \qquad \text{(A-7)}$$

where:

$$X = \frac{k \cot \psi}{\gamma}$$

$$k = \omega\sqrt{\mu\epsilon_o}$$

$$\eta = \frac{\mu}{\epsilon_o}$$

$$a = \cosh(\gamma\ell)$$

$$b = \sinh(\gamma\ell)$$

$$c = \sinh(\gamma s)$$

$$d = \cosh(\gamma s) \qquad \text{(A-8)}$$

At this point, it is convenient to simplify the calculations by breaking the problem into four cases of interest.

Case 1. Both circuits are wound in the same sense when viewed from above, or "parallel." Both circuits are also excited in-phase so that the radial component of E at the midplane is strong (++ mode). This is one of the useful modes for beam interaction. It is characterized by $B_1 = C_1 = 0$ in Eq. (A-4).

Case 2. Circuits are "crosswound" ($\psi_2 = -\psi_1$), (++ mode). This is also a potentially useful mode. For this case, $B_1 = D_1 = 0$.

Case 3. Circuits are parallel, excited out-of-phase (+—mode). This is not usually a useful mode for interaction since the electric fields are mainly transverse to the beam. However, because of mismatches at the circuit ends, this mode can produce parasitic resonances at discrete frequencies. For case 3, $A_1 = D_1 = 0$.

Case 4. Circuits are "crosswound," (+— mode). $A_1 = C_1 = 0$.

For case 1 ($B_1 = C_1 = 0$), Eq. (A-7) yields the following dispersion relationship:

$$X^2 = \frac{k^2 \cot^2 \psi}{\gamma^2} = \frac{\dfrac{b}{a} + \dfrac{d}{c}}{\dfrac{b}{a} + \epsilon' \dfrac{d}{c}} = \frac{\tanh(\gamma\ell) + \coth(\gamma s)}{\tanh(\gamma\ell) + \epsilon' \coth(\gamma s)} \qquad \text{(A-9)}$$

Equation (A-9) indicates that for no dielectric ($\epsilon' = 1$), the spiral circuit propagates waves in the radial direction at the "geometric" velocity, since $\gamma \equiv k \cot \psi$. With a thick dielectric, and wide circuit spacing, $\tanh(\gamma\ell)$ and $\coth(\gamma s)$ approach unity, so

$$\frac{v_p}{c} = \frac{k}{\gamma} = \sqrt{\frac{2}{\epsilon' + 1}} \tan \psi \qquad \text{(A-10)}$$

For all combinations of dimensions, the phase velocity is independent of the radius.

In a similar manner it is found that for case 2 (crosswound spirals):

$$X^2 = \frac{\coth(\gamma\ell) + \coth(\gamma s)}{\tanh(\gamma\ell) + \epsilon' \coth(\gamma s)} \tag{A-11}$$

For case 3 (parallel, transverse mode):

$$X^2 = \frac{\coth(\gamma\ell) + \coth(\gamma s)}{\coth(\gamma\ell) + \epsilon' \coth(\gamma s)} \tag{A-12}$$

For case 4:

$$X^2 = \frac{\tanh(\gamma\ell) + \coth(\gamma s)}{\coth(\gamma\ell) + \epsilon' \coth(\gamma s)} \tag{A-13}$$

Note that for cases 2 and 4, the wave does not propagate at the geometric velocity even if $\epsilon' = 1$.

A2. IMPEDANCE

The Pierce interaction impedance is defined as:

$$K = \frac{|E_r|^2}{2\gamma^2 P} \tag{A-14}$$

where:

E_r = radial component of electric field in the interaction region
P = rf power flowing radially

Values of γ are given by Eqs. (A-9) to (A-13). The power flow is given by:

$$P = 2\pi r \int_o^h \mathrm{Re}\,(E \times H^*)\,dr = 2\pi r \int_o^h \left(E_\theta H_z^* - E_z H_\theta^*\right) dr \tag{A-15}$$

The coefficients in Eqs (A-4) and (A-5) can be obtained from Eq. (A-7) for the appropriate case. For case 1:

$$A_2 = -A_1 \frac{a}{c}$$

$$D_1 = j \frac{A_1}{\eta X}$$

$$C_2 = -j \frac{A_1}{\eta X} \frac{a}{c} \tag{A-16}$$

Equation (A-15) then becomes:

$$P = 2\pi r A_1{}^2 R^2 \frac{k}{\eta\gamma}\left(\int_o^{\ell}\left\{\frac{1}{X^2}\cosh^2(\gamma z) + \sinh^2(\gamma z)\right\} dz\right.$$

$$\left. + \left(\frac{a}{c}\right)^2 \int_{\ell}^{h}\left\{\frac{1}{X^2}\sinh^2[\gamma(z-h)] \div \epsilon' \cosh^2[r(z-h)]\right\} dz\right) \quad \text{(A-17)}$$

$$= \frac{\pi r A_1{}^2 R^2 k}{\eta\gamma^2} \cdot Q \quad \text{(A-18)}$$

where:

$$Q = \gamma\ell\left(\frac{1}{X^2} - 1\right) + ab\left(\frac{1}{X^2} + 1\right) + \left(\frac{a}{c}\right)^2\left[\gamma s\left(\epsilon' - \frac{1}{X^2}\right) + cd\left(\epsilon' + \frac{1}{X^2}\right)\right] \quad \text{(A-19)}$$

so:

$$K = \frac{60\cosh^2(\gamma z)}{krQ} \quad \text{(A-19)}$$

For large spacings (or high frequencies) the impedance at the circuit ($z = \ell$) becomes:

$$K_{limit} = \frac{30}{kr(\epsilon' + 1)} \quad \text{(A-20)}$$

Similar expressions can be derived for the other cases. For case 2 (crosswound spirals) the value of Q for use in Eq. (A-19) is:

$$Q_2 = (ab - \gamma\ell)\left(\frac{a^2}{b^2X^2} + 1\right) + \left(\frac{a}{c}\right)^2\left[\gamma s\left(\epsilon' - \frac{1}{X^2}\right) + cd\left(\epsilon' + \frac{1}{X^2}\right)\right] \quad \text{(A-21)}$$

APPENDIX B
RADIAL WAVE-BEAM INTERACTION

Expressions for the interaction of a radial beam and a radial wave can be obtained in the same manner as for a helix and linear beam, keeping in mind that the rf field strength in the absence of the beam varies as $1/r$, and that the space-charge wavelengths of the beam are also functions of radius. If it is assumed that all rf quantities vary as

$$\exp\left(-\int_{r_1}^{r_2} \Gamma(r)\, dr\right)$$

then derivatives with respect to r can be replaced by $-\Gamma(r)$ times the quantity.

Following the method of Savel'yev,[4] the following determinental equation is obtained:

$$\left(-\Gamma(r) + j\Gamma_1 + \frac{1}{2r}\right)\left[\frac{4\beta_e p^2 C^3}{t} + \left(j\beta_e - \Gamma(r)\right)^2\right] + j\beta_e\beta_1{}^2 C^3 = 0 \qquad \text{(B-1)}$$

where:

$\Gamma_1(r) = \beta_1 - j\alpha_1$ = propagation constant of the circuit alone
$\beta_e = \omega/u_o$ = propagation constant of the beam
t = beam thickness
p = plasma frequency reduction factor
$C^3 = KI_o/4V_o$
I_o = dc beam current
V_o = voltage corresponding to the average electron velocity
K = interaction impedance evaluated at r

For convenience, $\Gamma(r)$ can be expressed in terms of the incremental propagation constant $\delta(r)$ as follows:

$$\Gamma(r) = j\beta_e\,[1 + jC\delta(r)]$$

$$= j\beta_e\left\{1 + jC\,[x(r) + jy(r)]\right\} \qquad \text{(B-2)}$$

Also:

$$\Gamma_1 = \beta_e(1 + Cb) - j\beta_e Cd \qquad \text{(B-3)}$$

where:

$$b = \frac{1}{C}\left(\frac{\beta_1}{\beta_e} - 1\right)$$

$$d = \frac{\alpha_1}{\beta_e C} \tag{B-4}$$

If we let

$$T = \frac{4p^2 C}{\beta_e t} \tag{B-5}$$

then Eq. (B-1) becomes:

$$\left[\delta(r) + jb + d + \frac{1}{2\beta_e C r}\right]\left[\delta^2(r) + T\right] + j\left(\frac{\beta_1}{\beta_e}\right)^2 = 0 \tag{B-6}$$

Except for the appearance of the $1/r$ term this expression is similar to that derived for a helix by Pierce, with T playing the part of $4QC$ in Pierce's analysis. Since Eq. (B-6) is of third order, there are three values of $\delta(r)$ for each combination of the other parameters. Usually, one of these will have a positive real part, indicating a wave that increases in amplitude with radius. This solution is customarily designated as $\delta_1 = x_1 + jy_1$. From the form of Eq. (B-6) it is seen that it is not possible to eliminate C, and that in fact, a "small C" solution has no meaning.

Solutions of Eq. (B-6) can be obtained by standard methods, using the formulas for cubic equations on the real and imaginary parts separately. This method can lead to some confusion in identifying the roots, so in the present case, the equation was solved in the complex δ plane, using a digital computer to evaluate successive approximations. Typical values of δ_1 for several values of C and T are shown in Figures B-1 and B-2.

The overall gain of the RBTWT depends on the division of input rf power among the three waves, which in turn depends on the operating parameters. Making the usual assumptions that at the tube input the ac velocity and ac current are zero, the following equations are obtained, assuming that the electric fields of the three waves add up to the applied field:

$$E_1 + E_2 + E_3 = E_T$$

$$E_1(\delta_1 + M) + E_2(\delta_2 + M) + E_3(\delta_3 + M) = 0$$

$$E_1\delta_1(\delta_1 + M) + E_2\delta_2(\delta_2 + M) + E_3\delta_3(\delta_3 + M) = 0 \tag{B-7}$$

where E_T is the total applied field and

$$M = jb + d + \frac{1}{2\beta_e C r_1} \tag{B-8}$$

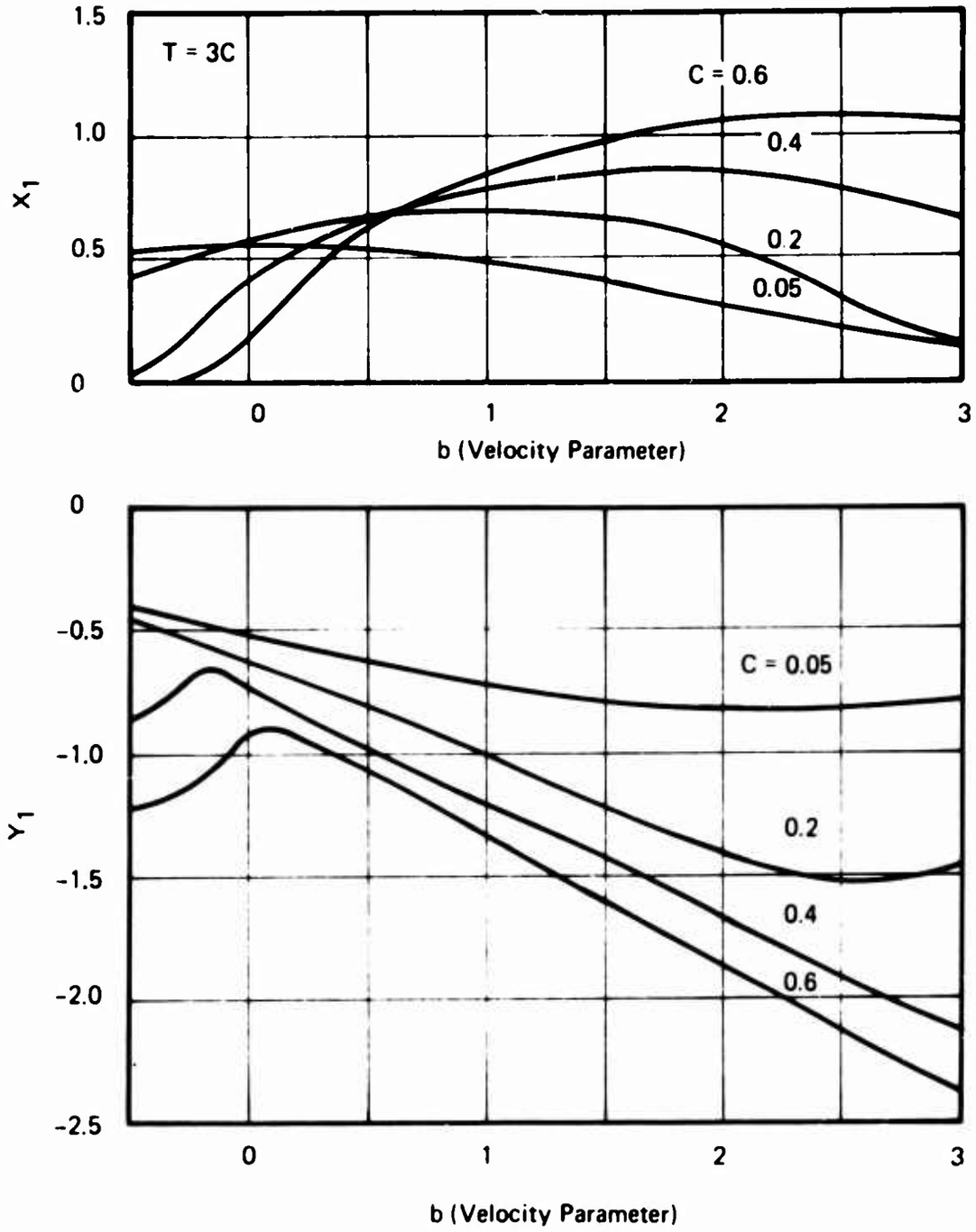

TP A-9538

Figure B-1. Incremental Propagation Constant δ_1.
($\beta e\, r = 10$)

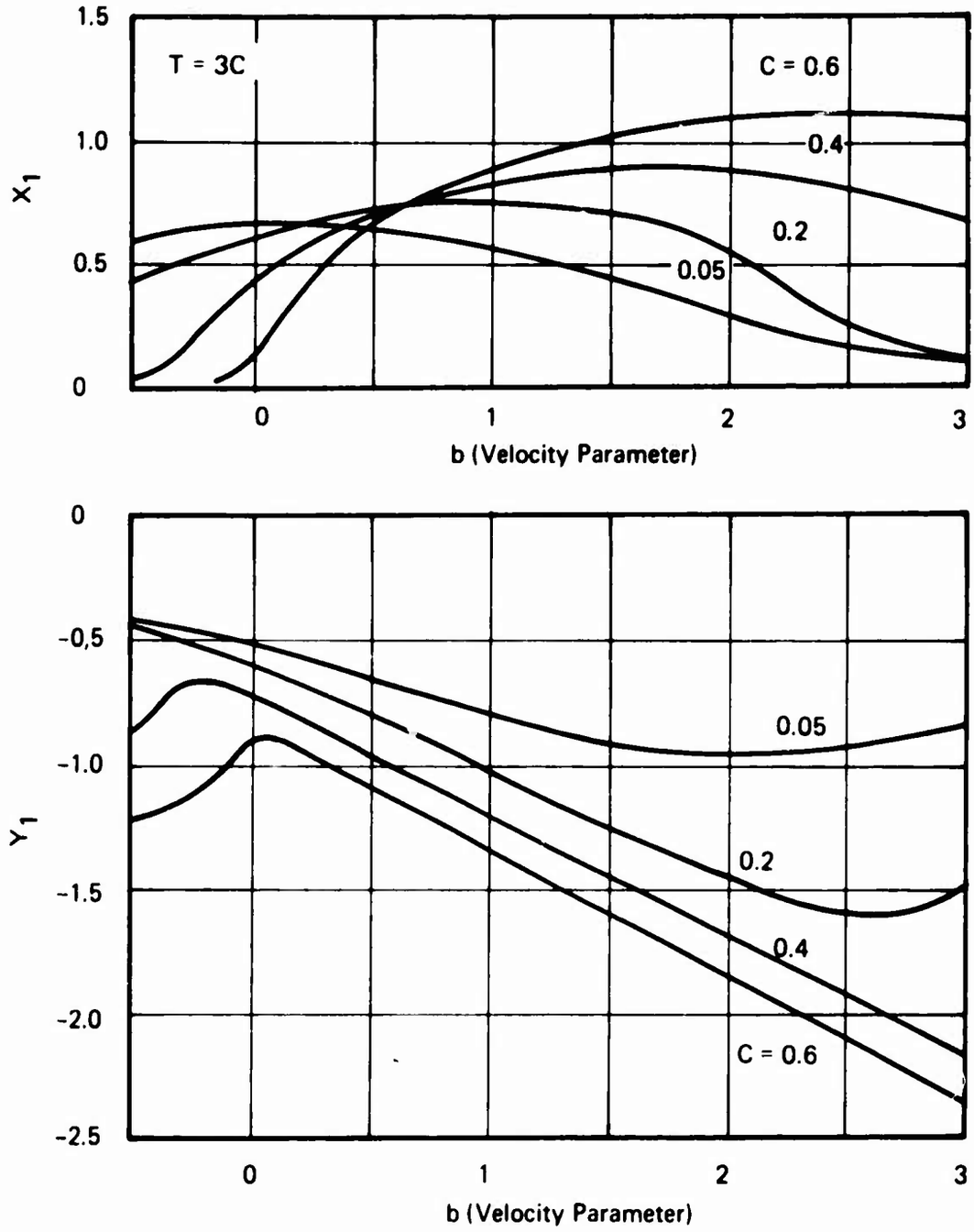

TP A-9539

Figure B-2. Incremental Propagation Constant δ_1.
($\beta e\, r = 20$)

Rearranging,

$$E_1 + E_2 + E_3 = E_T$$

$$E_1\delta_1 + E_2\delta_2 + E_3\delta_3 = -E_T M$$

$$E_1\delta_1^2 + E_2\delta_2^2 + E_3\delta_3^2 = E_T M^2 \qquad \text{(B-9)}$$

From which

$$\frac{E_1}{E_T} = \frac{\delta_2\delta_3 + M(\delta_2 + \delta_3) + M^2}{(\delta_1 - \delta_2)(\delta_1 - \delta_3)} \qquad \text{(B-10)}$$

Initial values for E_2 and E_3 are obtained from Eq. (B-10) by permuting subscripts. A "launching loss" can be defined as $20 \log |E_1/E_T|$ which then is the loss in dB incurred in setting up the growing wave. Typical values calculated from Eq. (B-10) are shown in Figure B-3(a).

It is also possible, and in some ways more logical, to define the launching loss in terms of the applied "voltage," where rf voltage is defined as E/Γ. If this is done, then using Eq. (B-2) the following expressions are obtained:

$$V_1 + V_2 + V_3 = V_T$$

$$V_1(1 + jC\delta_1)(\delta_1 + M) + V_2(1 + jC\delta_2)(\delta_2 + M) + V_3(1 + jC\delta_3)(\delta_3 + M) = 0$$

$$V_1(1 + jC\delta_1)^2(\delta_1 + M) + V_2(1 + jC\delta_2)^2(\delta_2 + M) + V_3(1 + jC\delta_3)^2(\delta_3 + M) = 0 \qquad \text{(B-11)}$$

From which

$$\frac{V_1}{V_T} \simeq \frac{E_1}{E_T}(1 + jC\delta_2)(1 + jC\delta_3) \qquad \text{(B-12)}$$

For small values of C, the difference between V_1/V_T and E_1/E_T is small, but because of the nature of δ_3, which tends to be purely imaginary and of order unity, $|V_1/V_T|$ can be much smaller than $|E_1/E_T|$ for large values of C. Typical values from Eq. (B-12) are shown in Figure B-3(b).

For purposes of the calculations in this report, the expression of Eq. (B-11) is used since it seems to fit the available experimental data better than Eq. (B-12). In an actual tube, the initial conditions are complicated by the fact that the circuit (and rf field) does not begin abruptly at a fixed radius. Local fringing fields between the circuit and adjoining electrodes produce some initial modulation which may aid or inhibit the effects produced later by the desired traveling wave fields.

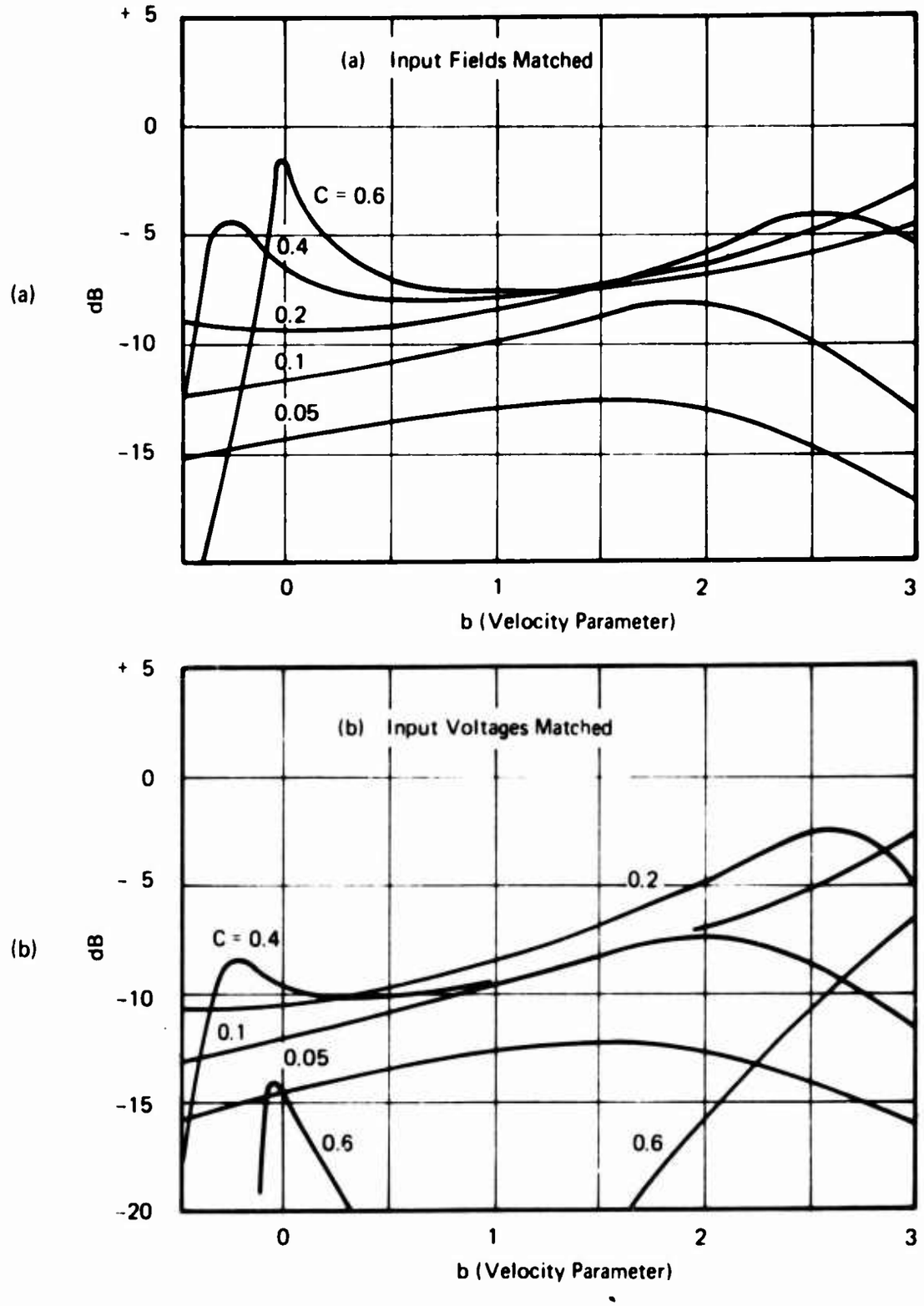

TP A-9540

Figure B-3. Launching Loss. The space charge parameter T = 3C, $\beta e\, r_1 = 10$, loss parameter d = 0.05.

APPENDIX C
IMPEDANCE REDUCTION FACTOR

Consider an electron just grazing a spiral circuit consisting of conducting arms of width w with spaces between conductors also of width w. Such an electron will alternately encounter zero field when it is above a conductor, and a fringing field between conductors. The interaction between such an electron and the field will be less than if the circuit were "smooth," as was assumed in the analysis of Appendix A.

A first approximation to the impedance reduction can be made by considering the fields to be made up of "space harmonic" components,[5] of which only the zero-order component is useful. This component is given by

$$E_o = \frac{E_r}{2w} \int_{-w/2}^{w/2} e^{j\gamma z}\, dz = E_r \left[\frac{\sin\left(\frac{\gamma w}{2}\right)}{\gamma w} \right] \tag{C-1}$$

where:

γ = radial propagation constant

E_r = radial field between conductors.

Evaluation of E_r requires solution of the complete boundary value problem including the conductor geometry, and will not be attempted here. Comparison with similar calculations for a tape helix[6] shows that the result depends to some extent on the assumed current distribution in the conductors, but in general, the impedance falls with increasing frequency and is very small when the phase shift between conductors is 2π. These same calculations show that the impedance is highest when the conductor and gap widths are equal.

The presence of the finite width conductors concentrates the field in the gaps, so the value of E_r in Eq. (C-1) is somewhat greater than that for the ideal spiral. For design purposes, it is assumed that the increase is a factor of $\sqrt{2}$. Since the impedance is proportional to the square of the field, an impedance reduction factor M can be defined as

$$M = 2 \left[\frac{\sin\left(\frac{\gamma w}{2}\right)}{\gamma w} \right]^2 \tag{C-2}$$

APPENDIX D
COMPUTER PROGRAM OUTLINE

The calculation of the gain of an RBTWT is best carried out with the aid of a digital computer because of the relatively large number of variables and the fact that the beam and circuit parameters vary with radius. The general approach involves dividing the radial interaction length into a number of segments (e.g., five) and calculating the beam and circuit parameters averaged over each segment. Starting at the input, the launching loss is calculated, then each of the three waves is followed to the end of the circuit. The integral appearing in Eq. (2-6) is evaluated by summing the product $\beta_e C\delta$ for each of the five segments. Each δ is calculated using the "local" values of C, d, beam velocity and space-charge parameter, averaged over the interval. At the output, the three waves are added vectorially and the gain calculated. The efficiency is estimated as being equal to twice the value of the gain parameter C at the output.

From the equations for phase velocity and impedance given in Appendix A, it is seen that the natural independent variable for use in calculations is $\gamma\ell$. However, calculations are usually desired at a fixed frequency, so an iterative process is required to "zero in" on the correct frequency, starting with an estimated value of $\gamma\ell$.

The flowchart of Figure D-1 shows the main features of the computer program used for this project. Figure D-2 is a typical computer printout.

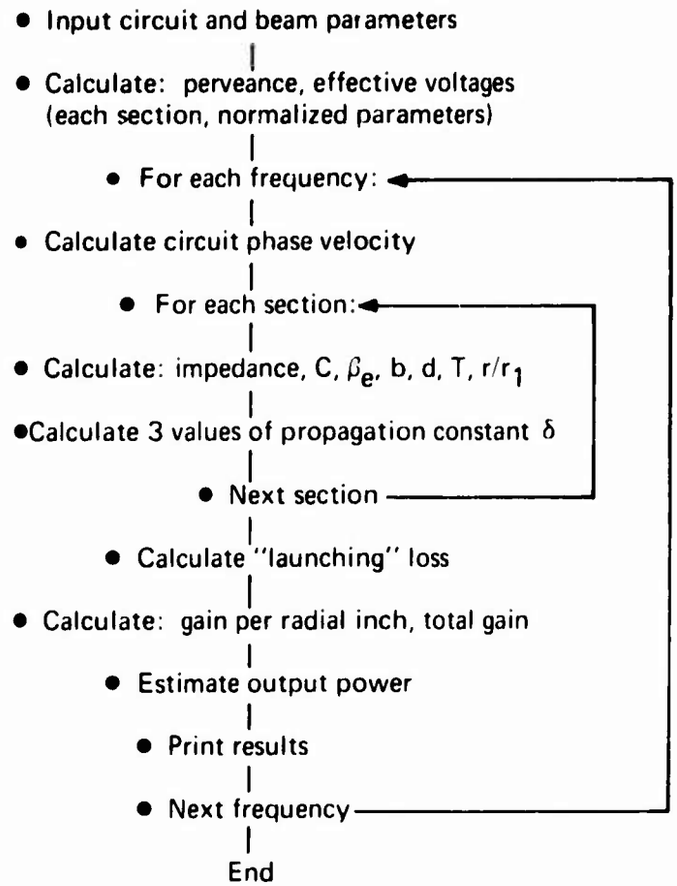

Figure D-1. Computer Flow Chart for Small Signal Gain Calculations

```
SMALL SIGNAL GAIN OF FLAT SPIRAL TWT -- REV I

SUBSTRATE DIELECTRIC CONST (REL)=6.6
PARALLEL- OR CROSS-WOUND (1,2) 1
N-FILAR N=2
UNIFORM SPIRAL (Y,N)? Y
SPIRAL CONSTANT= .042
CIRCUIT SPACING (IN)=.050
DIELECTRIC THICKNESS (IN)=.150
DIELECTRIC-SHIELD SPACING (IN)=0
INNER DIA (IN)=1.36
OUTER DIA (IN)=3.40
BEAM THICKNESS (IN)=.025
BEAM CURRENT (A)=2.5

LOWEST FREQ(GHZ)=.5
FREQ INTERVAL=.1
NO. POINTS=6

MAX USEFUL FREQ= 1041 MHZ

CURRENT DENSITY=  3.628 A/SQ CM AT INNER DIA
EST. LOSS AT   500 MHZ=   .36 DB

LOSS OK? (Y,N) Y

 ENTER CIRCUIT VOLTAGE (V)= 230

 EFF VOLTAGE (I/O)=  161.5 , 201.9
 U-PERV/SQ AT I.D.=   6.31 , FRACT VEL SPREAD=  .090
MIN FOCUSING FIELD=  785 GAUSS AT I.D. ( 470 AT O.D.)


FREQ GAIN(DB)  C-IN   C-OUT  B-IN/OUT  AI(DB) 'BCN'  XAV   N  2CIV(W)

 .50  12.77  .327  .210  1.11  2.49  -7.72  15.9  .681  1.6  212.5
 .60  13.16  .303  .190  1.12  2.62  -7.57  16.3  .636  1.9  191.4
 .70  13.03  .281  .171  1.13  2.77  -7.43  16.2  .590  2.3  172.6
 .80  12.50  .262  .154  1.15  2.95  -7.31  15.6  .541  2.6  155.5
 .90  11.91  .245  .138  1.17  3.16  -7.20  15.0  .501  2.9  139.8
1.00  11.12  .230  .124  1.19  3.41  -7.09  14.2  .461  3.2  125.4
```

Figure D-2. Typical Computer Printout